Contrib Mineral Petrol (2010) 160:865–885
DOI 10.1007/s00410-010-0511-5

ORIGINAL PAPER

Compositional variations in the Mesoarchean chromites of the Nuggihalli schist belt, Western Dharwar Craton (India): potential parental melts and implications for tectonic setting

Ria Mukherjee · Sisir K. Mondal · Minik T. Rosing · Robert Frei

Received: 6 October 2009 / Accepted: 2 March 2010 / Published online: 20 March 2010

Abstract The chromite deposits in the Archean Nuggihalli schist belt are part of a layered ultramafic–mafic sequence within the Western Dharwar Craton of the Indian shield. The 3.1-Ga ultramafic–mafic units occur as sill-like intrusions within the volcano-sedimentary sequences of the Nuggihalli greenstone belt that are surrounded by the tonalite–trondhjemite–granodiorite (TTG) suite of rocks. The entire succession is exposed in the Tagdur mining district. The succession has been divided into the lower and the upper ultramafic units, separated by a middle gabbro unit. The ultramafic units comprise of deformed massive chromitite bodies that are hosted within chromite-bearing serpentinites. The chromitite bodies occur in the form of pods and elongated lenses (~60–500 m by ~15 m). Detailed electron microprobe studies reveal intense compositional variability of the chromite grains in silicate-rich chromitite (~50% modal chromite) and serpentinite (~2% modal chromite) throughout the entire ultramafic sequence. However, the primary composition of chromite is preserved in the massive chromitites (~60–75% modal chromite) from the Byrapur and the Bhaktarhalli mining district of the Nuggihalli schist belt. These are characterized by high Cr-ratios (Cr/(Cr + Al) = 0.78–0.86) and moderate Mg-ratios (Mg/(Mg + Fe^{2+}) = 0.38–0.58). The compositional variability occurs due to sub-solidus re-equilibration in the accessory chromite in the serpentinite (Mg-ratio = 0.01–0.38; Cr-ratio = 0.02–0.99) and in silicate-rich chromitite (Mg-ratio = 0.06–0.48; Cr-ratio = 0.60–0.99). In the massive chromitites, the sub-solidus re-equilibration for chromite is less or absent. However, the re-equilibration is prominent in the co-existing interstitial and included olivine ($Fo_{96–98}$) and pyroxene grains (Mg-numbers = 97–99). Compositional variability on the scale of a single chromite grain occurs in the form of zoning, and it is common in the accessory chromite grains in serpentinite and in the altered grains in chromitite. In the zoned grains, the composition of the core is modified and the rim is ferritchromit. In general, ferritchromit occurs as irregular patches along the grain boundaries and fractures of the zoned grains. In this case, ferritchromit formation is not very extensive. This indicates a secondary low temperature hydrothermal origin of ferritchromit during serpentinization. In some occurrences, the ferritchromit rim is very well developed, and only a small relict core appears to remain in the chromite grain. However, complete alteration of the chromite grains to ferritchromit without any remnant core is also present. The regular, well-developed and

Communicated by T. L. Grove.

Electronic supplementary material The online version of this article (doi:10.1007/s00410-010-0511-5) contains supplementary material, which is available to authorized users.

R. Mukherjee · S. K. Mondal
Department of Geological Sciences,
Jadavpur University, Kolkata 700032, India

S. K. Mondal (✉) · M. T. Rosing · R. Frei
Nordic Center for Earth Evolution,
Natural History Museum of Denmark,
University of Copenhagen, Øster Voldgade 5-7,
1350 Copenhagen, Denmark
e-mail: sisir.mondal@gmail.com; skmondal@snm.ku.dk

S. K. Mondal
Department of Earth and Planetary Sciences,
American Museum of Natural History,
Central Park West@79th Street, New York, NY 10024, USA

R. Frei
Institute of Geography and Geology, University of Copenhagen,
Øster Voldgade 10, 1350 Copenhagen, Denmark

continuous occurrence of ferritchromit rims around the chromite grain boundaries, the complete alteration of the chromite grains and the modification of the core composition indicate the alteration in the Nuggihalli schist belt to be intense, pervasive and affected by later low-grade metamorphism. The primary composition of chromite has been used to compute the nature of the parental melt. The parental melt calculations indicate derivation from a high-Mg komatiitic basalt that is similar to the composition of the komatiitic rocks reported from the greenstone sequences of the Western Dharwar Craton. Tectonic discrimination diagrams using the primary composition of chromites indicate a supra-subduction zone setting (SSZ) for the Archean chromitites of Nuggihalli and derivation from a boninitic magma. The composition of the komatiitic basalts resembles those of boninites that occur in subduction zones and back-arc rift settings. Formation of the massive chromitites in Nuggihalli may be due to magma mixing process involving hydrous high-Mg magmas or may be related to intrusions of chromite crystal laden magma; however, there is little scope to test these models because the host rocks are highly altered, serpentinized and deformed. The present configurations of the chromitite bodies are related to the multistage deformation processes that are common in Archean greenstone belts.

Keywords Chromite · Ferritchromit · Komatiite · Boninite · Subduction zone · Archean greenstone belt · Dharwar Craton · India

Introduction

The study of the Archean greenstone belts is important because they represent some of the earliest records of Earth's lithospheric history (e.g., de Wit and Ashwal 1995). The ultramafic and mafic rocks within the greenstone belts are a key focus of study as they host economically important deposits such as chromite, nickel–copper sulfides, titaniferous–vanadiferous magnetite and platinum group elements (e.g., Mondal 2009). The chromitite bodies within the ultramafic rocks of the greenstone belts are of particular importance and interest, because all the other rocks of the sequence are heavily serpentinized, deformed and metamorphosed.

Composition of chromite in different deposits is characteristically distinct and diverse, which is a function of parental melt compositions generated in different tectonic settings (e.g., Dick and Bullen 1984; Kamenetsky et al. 2001 and references therein). Chromite can be used efficiently as a guide to understand the tectonic and the crust-mantle processes that operated in the Archean Earth, because it preserves geochemical signatures of its source magmas (Stowe 1994; Rollinson 1995a; Mondal et al. 2006). The petrogenetic and tectonic inferences are always based on studies from massive chromitite as they successfully retain the pristine composition (e.g., Mondal et al. 2006). Compositional variability is very common in accessory chromites (e.g., Irvine 1965, 1967; Jackson 1969; Roeder et al. 1979) and may arise due to sub-solidus re-equilibration of the chromite with surrounding silicate minerals and interstitial melt (e.g., Hamlyn and Keays 1979; Scowen et al. 1991; Rollinson 1995b). Oxidation and alteration of chromite to ferritchromit with magnetite rims is also commonly observed in both alpine-type ultramafic complexes as well as in komatiitic rocks (e.g., Barnes 2000) and is related to serpentinization of the host rock and its subsequent metamorphism (Evans and Frost 1975; Bliss and Maclean 1975; Loferski and Lipin 1983; Burkhard 1993; Abzalov 1998).

The chromitites of the Archean greenstone belts are hosted within sill-like intrusions of ultramafic bodies and are thought to be genetically linked to komatiitic magmas. Typical example includes the chromitite of the Shurugwi greenstone belt in Zimbabwe (Stowe 1987; Rollinson 1997; Prendergast 2008). Similar examples occur in the Indian shield and include the Mesoarchean Nuasahi–Sukinda–Jojohatu complexes within the Iron Ore Group greenstone belts of the Singhbhum Craton (e.g., Mondal et al. 2001) and the Archean Nuggihalli–Krishnarajpet–Holenarsipur–Nagamangala–Javanhalli greenstone belts of the Western Dharwar Craton (e.g., Radhakrishna and Vaidyanadhan 1994).

The chromite deposits of India account for ~18% of world production (Papp 2008). Among these, the Nuasahi–Sukinda complexes in eastern India account for ~95% of the total Indian production. Minor chromium resources occur in southern India. The resources are mainly represented by the Archean chromite deposits of the Nuggihalli schist belt (Fig. 1). The chromitite bodies in the Nuggihalli schist belt occur as dismembered lenses within highly deformed and serpentinized dunite (Ramakrishnan 1981; Nijagunappa and Naganna 1983). The chromite-bearing ultramafic bodies are layered and are surrounded by the tonalite–trondjhemite–granodiorite (TTG) suite of rocks (Radhakrishna 1983; Jafri et al. 1983). Previous works mainly focused on the mineralogical studies of chromite from the chromitites of the Nuggihalli schist belt; there are some studies on the associated secondary mineral assemblages of the serpentinized peridotite from the ultramafic bodies as well (Damodaran and Somasekar 1976; Mitra et al. 1992; Mitra and Bidyananda 2001; Devaraju et al. 2007). Bidyananda and Mitra (2005) had inferred a komatiitic affinity for the Nuggihalli chromitite. However, this conclusion is based on limited analytical data of chromite from a single mining district.

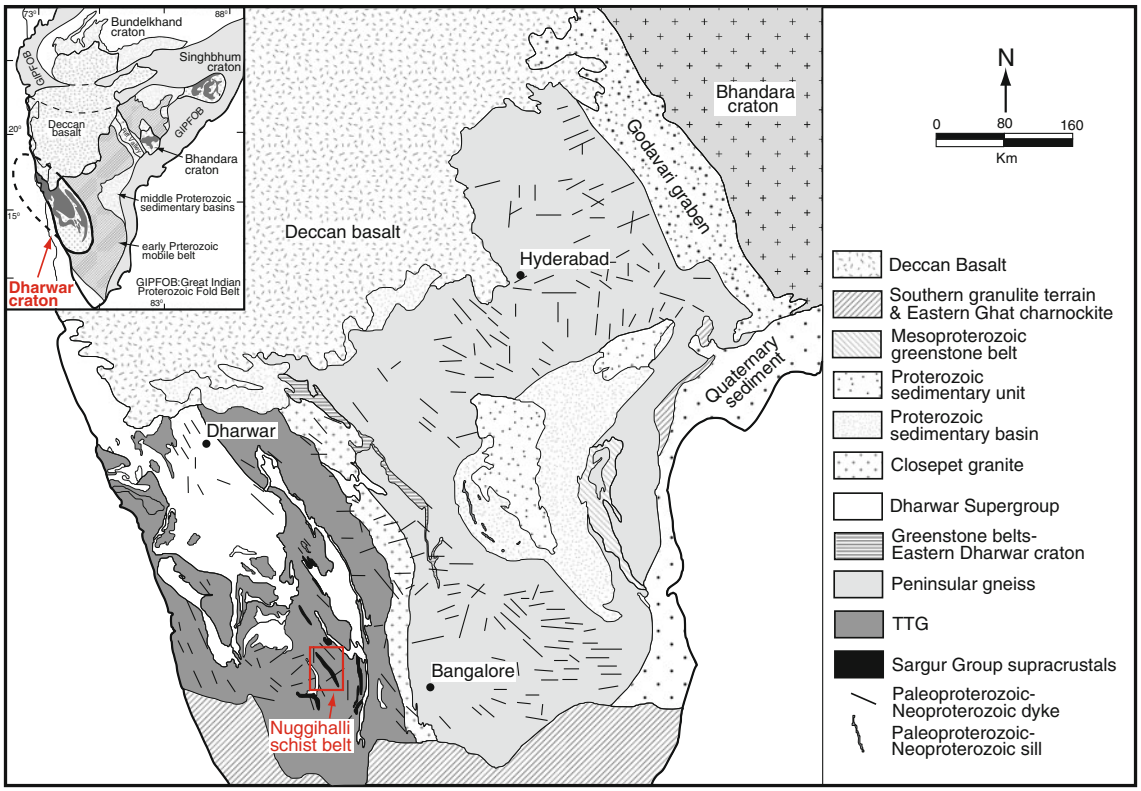

Fig. 1 Generalized geology of the Dharwar Craton showing location of the Nuggihalli schist belt (after Murthy 1987; cited in Devaraju et al. 2009). *Inset* map is the generalized geology of the Indian shield showing Dharwar Craton (compiled by Mondal et al. 2006; after Radhakrishna and Naqvi 1986; Leelananadam et al. 2006)

Detailed characterization of the chromites and their compositional variability have not been addressed before from this area, and it is essential, as these rocks are part of a deformed, altered and metamorphosed Archean greenstone sequence, where compositional variability is expected within the minerals including chromite. Hence, this aspect has to be meticulously studied before using chromite as a petrogenetic tool. In this study, detailed investigation into the chromitite deposits of the Nuggihalli schist belt has been carried out by systematic sampling from different mine sections (both underground and open cut) and outcrops, and, by using petrographic and mineral analyses. The main goal of this study is to characterize the chromite from petrographic and mineralogical studies in order to understand the parental magma character, the genesis, subsolidus history and other secondary processes that may have acted upon the chromite grains, thereby inducing variability in their composition.

Regional geological setting

The Nuggihalli schist belt is situated in the western part of the Dharwar Craton (Fig. 1). The Dharwar Craton is subdivided into the Western Dharwar Craton and the Eastern Dharwar Craton by a 500 km long lineament of alkali feldspar-rich granite known as the Closepet granite (e.g., Gupta et al. 2003; Naqvi 2005). The Western Dharwar Craton is composed of older supracrustals known as the Sargur Group (3.3–3.1 Ga) that are enclosed within the associated tonalite–trondhjemite–granodiorite (TTG) suite (Fig. 1). The older supracrustals are succeeded by younger supracrustals of the Dharwar Supergroup (2.8–2.6 Ga) that rest uncomformably over the TTG. The supracrustals of the Dharwar Supergroup are subsequently intruded by the 2.5-Ga Closepet granite. The rocks in the Nuggihalli schist belt belong to the Sargur Group. The Sargur Group of rocks occur as linear ultramafic–mafic belt, containing minor clastic sediments and banded iron formation (BIF), in the Nuggihalli area (Fig. 2). The ultramafic–mafic rocks of the Sargur Group occur both as intrusive bodies as well as volcanics (Ramakrishnan 2009). Compositionally, the ultramafic rocks that represent the schist belt are komatiitic, and the mafic rocks are compositionally tholeiitic to komatiitic basalt. The supracrustals of the Sargur Group are intensely deformed and metamorphosed from greenschist to amphibolite facies. Three phases of deformation are recognized—one that developed schistocity parallel to the bedding, the second that developed upright tight to isoclinal folds and the third that folded the earlier regional fold

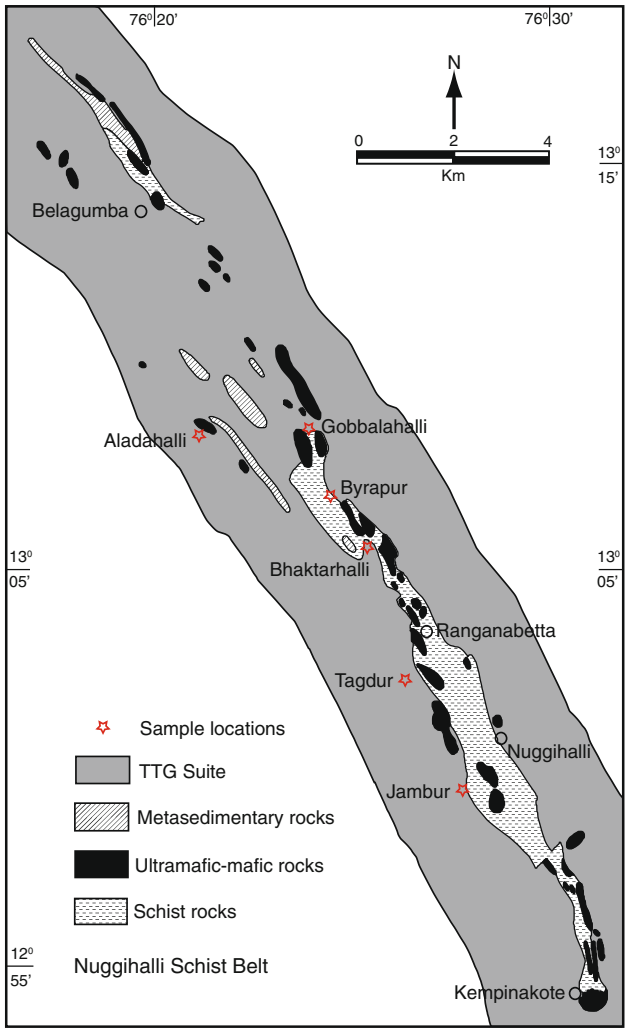

Fig. 2 Geology of the Nuggihalli schist belt showing locations of the chromite mining districts (after Jafri et al. 1983; cited in Devaraju et al. 2009). Sample locations are marked

to a north or northeast trend (Radhakrishna and Vaidyanadhan 1994).

Bidyananda et al. (2003) had obtained a $^{207}Pb/^{206}Pb$ zircon age of 3.3 Ga for the metasediments of the Nuggihalli schist belt. The gneisses of the TTG suite in Nuggihalli have zircon ages ranging from 3.0 to 3.3 Ga (Bidyananda et al. 2003). Recently, Jayananda et al. (2008) have dated the age of the komatiitic suite from the schist belt using Sm–Nd whole rock isochron to 3,352 ± 110 Ma. Using the Pb–Pb whole rock isochron method, Mondal et al. (2008) have found the age to be 3,156 ± 170 Ma for the entire ultramafic–mafic succession of the Nuggihalli schist belt that includes samples of peridotite, chromitite, gabbro and ultramafic–mafic schist rocks. This age is correlative with the $^{207}Pb/^{206}Pb$ zircon age of 3.1 Ga of the surrounding TTG suite as determined by Bidyananda et al. (2003). The contact between the Sargur Group and surrounding TTG is obscure, and in parts, the boundary has also been migmatized; their stratigraphy cannot be established from field relations.

Geology of chromitite deposits of the Nuggihalli schist belt

The Nuggihalli schist belt represents a linear belt trending NNW–SSE, with a length of 60 km and a maximum width of 2 km (Fig. 2). The chromiferous ultramafic rocks of the Nuggihalli schist belt occur as discontinuous *en echelon* and lenticular bodies and were originally part of a narrow, sill-like ~250-km-long layered ultramafic–mafic intrusion within the volcano-sedimentary greenstone sequences (Figs. 1, 2). Main rock types of the chromite-bearing ultramafic bodies include dunite and pyroxenite that are extensively serpentinized. In addition, an anorthosite band is present within the ultramafic body of the Jambur mining district.

The chromiferous ultramafic bodies are exposed both in open pit and underground workings in the Hassan district of Karnataka state. Byrapur is the largest chromite mine that is presently operating in Karnataka with a total depth of ~305 m (Fig. 2). The entire layered ultramafic–mafic succession is well preserved in the Tagdur mining district (Fig. 2). The ultramafic–mafic succession has been divided into three major units: (1) the lower ultramafic unit, (2) middle gabbro and (3) upper ultramafic unit. The chromitite bodies occur in both the lower and the upper ultramafic units. The chromitite bodies are lenticular (length ~60–500 m and width ~15 m). There are various different shapes and dispositions observed for the chromitite body-like pod, elongated band, lenses, stringers and folded chromitite (Fig. 3). The main chromitite body in Byrapur appears to be sack shaped, laterally impersistent (pinches out) and vertically extended. The trend of the chromitite body in Nuggihalli is found to vary from N–S through NE–SW to E–W with a dip of 60°–80°. The chromitite body within the upper ultramafic unit is elongated and lenticular with a trend of NNW–SSE and dip of 70°–80° toward west. Contacts between the chromitite body and the host serpentinite are highly sheared.

The contact between the rocks of the lower ultramafic unit and the middle gabbro is not exposed in Tagdur area. Bands of conformable massive magnetite are located at the lower and uppermost parts of the middle gabbro. The gabbro shows modal layering and is anorthositic at the upper part. At Tagdur, the surrounding schist rocks (Fig. 2) include fine-grained amphibolite schist, tremolite–actinolite–quartz–chlorite schist, chlorite–sericite schist and metagabbro with variable modes of magnetite, ilmenite and hematite.

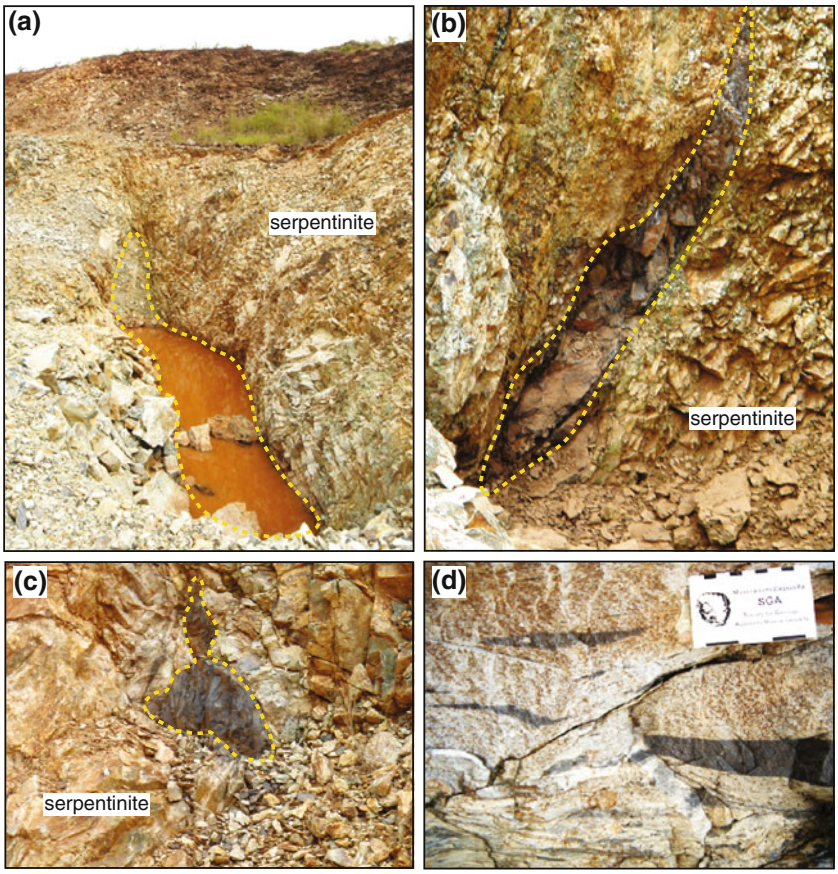

Fig. 3 Photographs showing various different shapes and dispositions of chromitite ore bodies in the Nuggihalli schist belt. **a** Sigmoidal-shaped chromitite ore body (mined out; maximum length ~15 m and maximum width ~5 m) hosted within deformed serpentinite; chromitite from lower ultramafic unit, Tagdur. **b** Lens-shaped chromitite ore body (maximum length ~3 m); chromitite from lower ultramafic unit, Tagdur. **c** Small pod-shaped chromitite (maximum length ~0.5 m); chromitite from lower ultramafic unit, Tagdur. **d** Stringers of folded chromitite lenses, Bhaktarhalli

Sampling and analytical work

Samples were collected with the aim to study chromite occurrences in different rocks so that spatial as well as lithological controls on chromite composition can be investigated (Fig. 2). The samples were collected from the open cut and underground mines, as well as from outcrops showing different textures, so that compositional variability related to mode could be studied. All samples collected from the field were studied in hand specimen and in thin-polished sections using both transmitted and reflected light microscopes. Chromite grains along with interstitial and included silicate mineral phases were analyzed by electron microprobe using a JEOL JXA–8600 superprobe instrument at the Institute of Geography and Geology, University of Copenhagen, operated at 15-kV acceleration voltage with 20-nA probe current, using natural mineral standards and standard ZAF matrix corrections. The complete dataset is provided as an Electronic Appendix, which can be downloaded from http://www.editorialmanager.com/comipe/download.aspx?id=43346&guid=f6dae76a-aa83-4378-81ca-4ebc24f5cf97&scheme=1. The compositions of chromite are recalculated to cation proportions using the Fe^{3+} calculation scheme of Droop (1987).

Description of chromite-bearing rocks

Serpentinized dunite

Dunite is extensively altered to serpentinite (Fig. 3); however, primary cumulate textures of the protolith are sometimes preserved. The rock is highly deformed and veined by magnesite and cryptocrystalline silica. In the more deformed parts, the rock exhibits at least two sets of schistocity in the N–S and NW–SE direction. Antigorite is the major constituent in serpentinite along with minor lizardite. Micro-veins of chrysotile often cut across antigorite. Serpentinite mostly exhibits interpenetrating, mesh and pseudomorph textures. Flakes of chlorite occur in the matrix that are sheared and are further altered along the cleavage planes to form second-generation chlorite. Coarser flakes of chlorite show development of kink bands. There are also irregular patches of magnesite that are enclosed by flakes of antigorite. Minor tremolite occurs as long-bladed prismatic grains elongated along the schistocity. Chromite occurs as an accessory mineral in the serpentinite. Small discrete grains of magnetite develop as secondary oxides during serpentinization and are either concentrated in the serpentine veins or are scattered

throughout the rock in general. Sulfide minerals (mainly chalcopyrite) are observed as small minute spherical grains scattered within the serpentinite.

Metapyroxenite

The rock is poorly exposed at Tagdur but has been reported from other localities of the belt such as from Byrapur (e.g., Radhakrishna 1996). Earlier workers (e.g., Ramakrishnan 1981; Jafri et al. 1983) described the pyroxenites, metamorphosed to talc–actinolite–tremolite–chlorite schist, to be occurring along with dunite as discontinuous lenses. At Tagdur, the metapyroxenite is present in between the chromiferous lower ultramafic unit and the middle gabbro. It shares sheared and conformable contact with the lower magnetite bands of the middle gabbro. The rock is composed of chlorite, actinolite and minor quartz. Common accessory phases include altered chromite, magnetite and ilmenite. The rock lacks an overall fabric where all grains are randomly oriented. Actinolite occurs as long prismatic blades. Few coarse grains of orthopyroxene (hypersthene) are also present. Chlorite occurs as laths and cut across actinolite and hypersthene grains.

Chromitite

The chromitite (~60–75% modal chromite) in Nuggihalli exhibits primary igneous layering where individual seams contain layers of massive, spotted, schlieren-banded and net-textured chromitite (Fig. 4). At Byrapur, the massive chromitite contains clots that are enriched in silicate minerals. The chromite within the clots is fine grained compared to the overall rock. The massive chromitite contains relict olivine and pyroxene grains that are interstitial to chromite grains, and therefore, they are relatively fresh and unaltered compared to the massive chromitite of Tagdur. The modes of altered silicate minerals vary to considerable degrees (~10–50%) in the massive chromitite at Tagdur. Chromite contains inclusions of primary silicate minerals that are spherical to euhedral in shape and are of orthopyroxene, olivine and clinopyroxene (Figs. 5a, 6a). The inclusion minerals are often altered to serpentine-, chlorite- and magnesite-bearing assemblages.

Lamellar chrome–chlorite (kaemmererite) is a common associate in the altered assemblage of chromitite. Chlorite usually occurs as veining material within the chromite as well as along the grain boundary. Magnesite occurs as micro-veins within the chromite and at places they transgress antigorite. Minor amount of sulfide minerals (pentlandite and millerite) are present within the interstitial spaces while a few are included within the chromite grains. The interstitial serpentines in the chromitite mostly show interpenetrative and interlocking textures. Few of the serpentine veins within chromitite exhibit displacement indicating that the rock has suffered some shearing after serpentinization.

Fig. 4 Photographs of hand specimens illustrating different textures in chromitite. **a** Chromitite exhibits primary layering and shows transition from massive chromitite to schlieren-banded chromitite; upper ultramafic unit, Tagdur. **b** Primary igneous inter-layering of serpentinized dunite and chromitite; schlieren-banded (*left*) and spotted chromitite (*right*); Bhaktarhalli

Textural characteristics of chromite

Chromite is present in serpentinized ultramafic rocks as an accessory phase (Figs. 5b, d, 6d) and in chromitite as a major constituent (Figs. 5a, c, e, f, 6a–c). Accessory chromite grains are subhedral to subrounded in shape, have corroded margins and are surrounded by a halo of chrome–chlorite. The chromite grains occur in clusters and are broken and granulated to smaller fragments that are disseminated through out the serpentinized matrix, owing to deformation. The accessory chromite grains in the serpentinite are smaller in size compared to the grains in the massive chromitite. In the massive chromitite from the

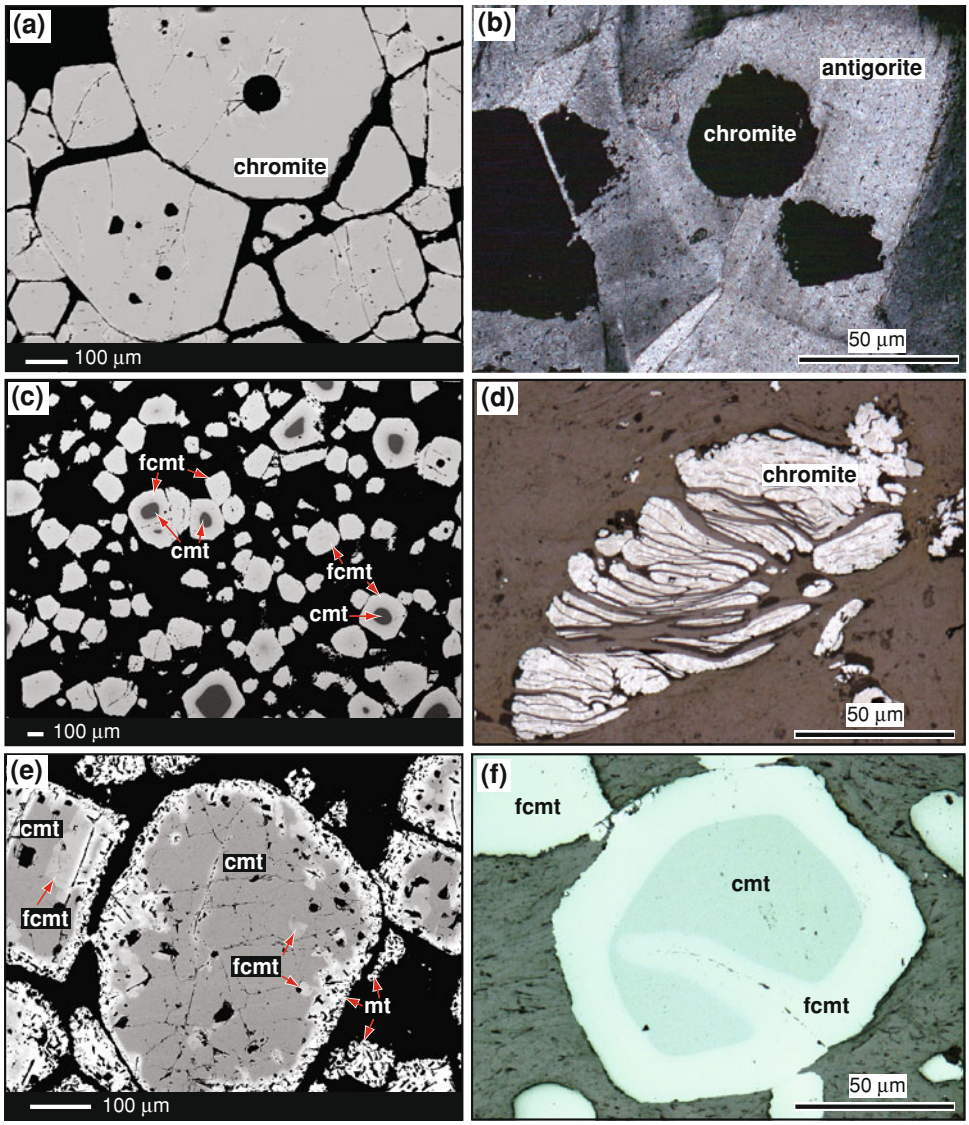

Fig. 5 **a** Back-scattered electron (BSE) image of primary chromites with silicate inclusions; interstitial materials (*black*) are serpentine and chlorite; massive chromitite, Byrapur, sample 27a. **b** Optical image showing accessory chromite in serpentinite with corroded grain boundary set in a matrix of antigorite; transmitted light between crossed nicols; serpentinite, Gobbalahalli, sample GH3. **c** BSE image of compositionally zoned chromite, central darker portion (*core*) is remnant chromite (*cmt*) surrounded by brighter ferritchromit rim (*fcmt*), some grains are homogeneously altered to ferritchromit (*fcmt*); interstitial materials (*black*) are serpentine and chlorite; chromitite with high silicate mode, Jambur, sample JM6. **d** Optical image of oxidized and deformed accessory chromite grain in serpentinite; reflected light; serpentinite, Tagdur, sample TD6. **e** BSE image of zoned chromite, altered core (*cmt*) with heterogeneous patches of ferritchromit (*fcmt*) and magnetite rim (*outer brighter most rim*), smaller grains are homogenously altered to magnetite (*mt*); interstitial *black* materials are serpentine, chlorite and magnesite; schlieren-banded chromitite, upper ultramafic unit, Tagdur, sample 40b. **f** Optical image of zoned chromite with ferritchromit (*fcmt*) formation around rim and also along fracture; reflected light; chromitite with high silicate mode, Jambur, sample JM6

upper ultramafic unit of Tagdur, the boundaries of the chromite grains are highly corroded, and overall the cumulus grains exhibit a skeletal texture. The chromite grains of the schlieren-banded and spotted chromitite of the upper ultramafic unit in Tagdur, have higher reflectance compared to the massive chromitite of the lower ultramafic unit, because of intense alteration. At Byrapur, the chromites in massive chromitite are coarse grained, euhedral, exhibit polygonal appearance and are less deformed (Figs. 5a, 6a).

In reflected light and in scanning electron microscopic (SEM) study, the accessory chromite grains in serpentinite, and the altered grains in massive chromitite and in silicate-rich chromitite, commonly exhibit strong compositional zoning (Figs. 5c, e, f, 6b–d). The central part or core of the grain is darker than the outer rim which is lighter gray in

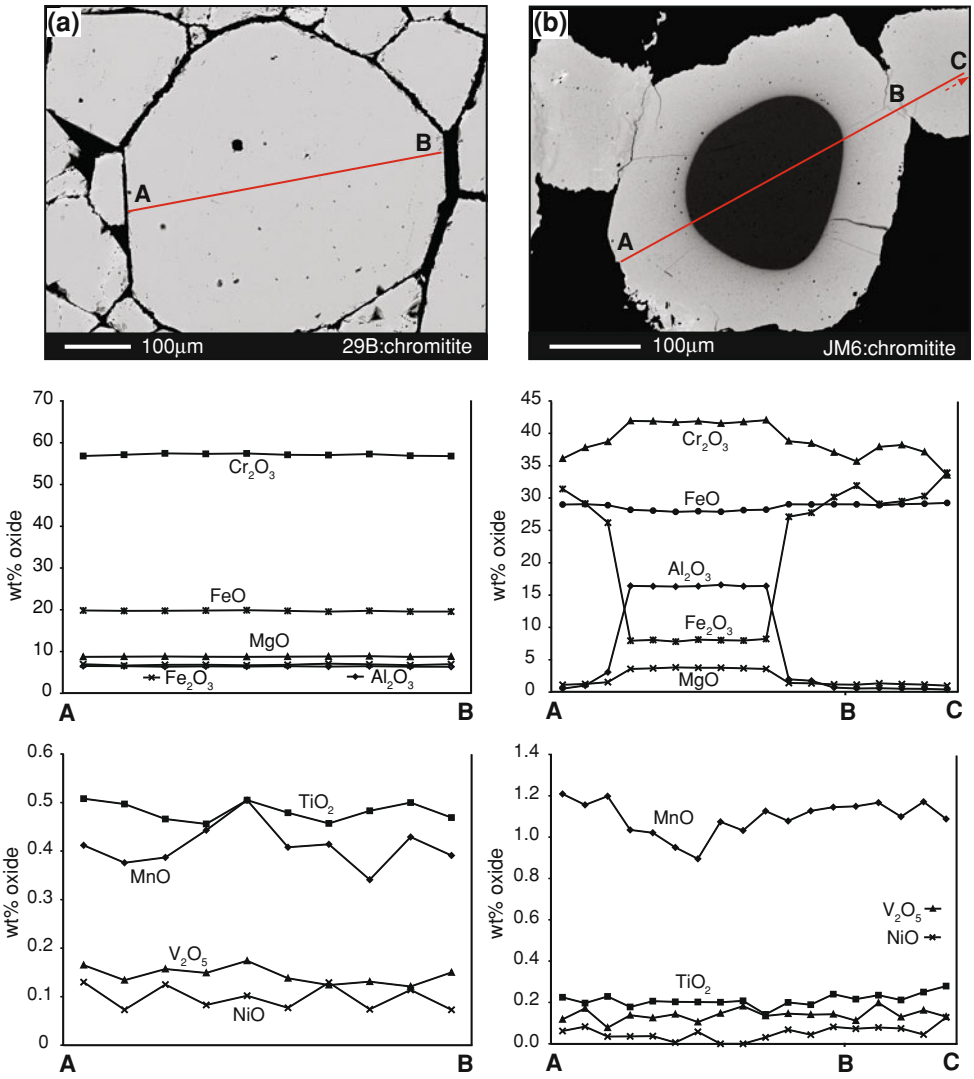

Fig. 6 Quantitative microprobe profiles of major and minor elements across zoned and unzoned chromite grains. **a** BSE image of unzoned chromite from Byrapur showing microprobe traverse A–B; no variation is observed for major elements; sample 29B, massive chromitite. **b** BSE image of zoned chromite showing microprobe traverse A–B–C over the zoned grain and the adjoining optically homogeneous grain; loss of Cr–Al is compensated by enrichment of Fe^{3+} and loss of Mg by enrichment of Mn in the grain; optically homogeneous grain is chemically altered with loss of Cr made up by intake of Fe^{3+} in the grain; sample JM6, silicate-rich chromitite. **c** BSE image of zoned chromite showing microprobe traverse A–B; zoning is gradational with loss of Cr–Al–Mg being compensated by intake of Fe^{2+}–Fe^{3+}–Ti–Mn in the grain; sample GH1, massive chromitite. **d** BSE image of zoned accessory chromite in serpentinite showing microprobe traverse A–B; loss of Cr–Al–Mg is compensated by intake of Fe^{3+}–Ti–Mn in the grain; sample 23, serpentinite

color and has a higher reflectance. The more highly reflecting areas often occur as small irregular patches or along the fractures within the grain such as in the chromitite of the upper ultramafic unit of Tagdur (Fig. 5e, f). Occasionally, accessory chromite and chromite from the extensively altered massive chromitite (such as from Gobbalahalli, Tagdur, Jambur, Aladahalli; Fig. 2) show the development of two outer rims instead of the usual one. Here, the outer rim of the highest reflectance surrounds the inner rim which is lighter gray in color. The central part is identified as remnant, unaltered chromite, the inner rim is of ferritchromit, whereas the outer rim is identified as magnetite. The outer rim has highly irregular contacts with the surrounding chlorite. Magnetite occurs along the grain boundary in a continuous or discontinuous manner (Fig. 5e), along the fractures within the grains, and, is rare in occurrence compared to ferritchromit. In some extensively altered parts of chromitite, most of the grains are completely modified to ferritchromit. Only a few grains contain remnants of chromite at the core (Figs. 5c, 6b); these grains show well-developed, regular and continuous ferritchromit rims that surround the core. The smaller broken chromite grains are completely oxidized to ferritchromit and magnetite compared to the larger cumulus grains (Figs. 5c, e, f, 6b).

Mineral compositions

Olivine and pyroxene

Olivine grains are highly magnesian in the Nuggihalli chromitite (Electronic Appendix). The olivine inclusions exhibit slightly higher Mg values ($Fo_{97–98}$) compared to the interstitial grains ($Fo_{96–97}$). We will argue that the high Mg contents of the olivine grains indicate loss of Fe to the host chromite during alteration and metamorphism. Bidyananda and Mitra (2005) had reported relict olivine grains in the

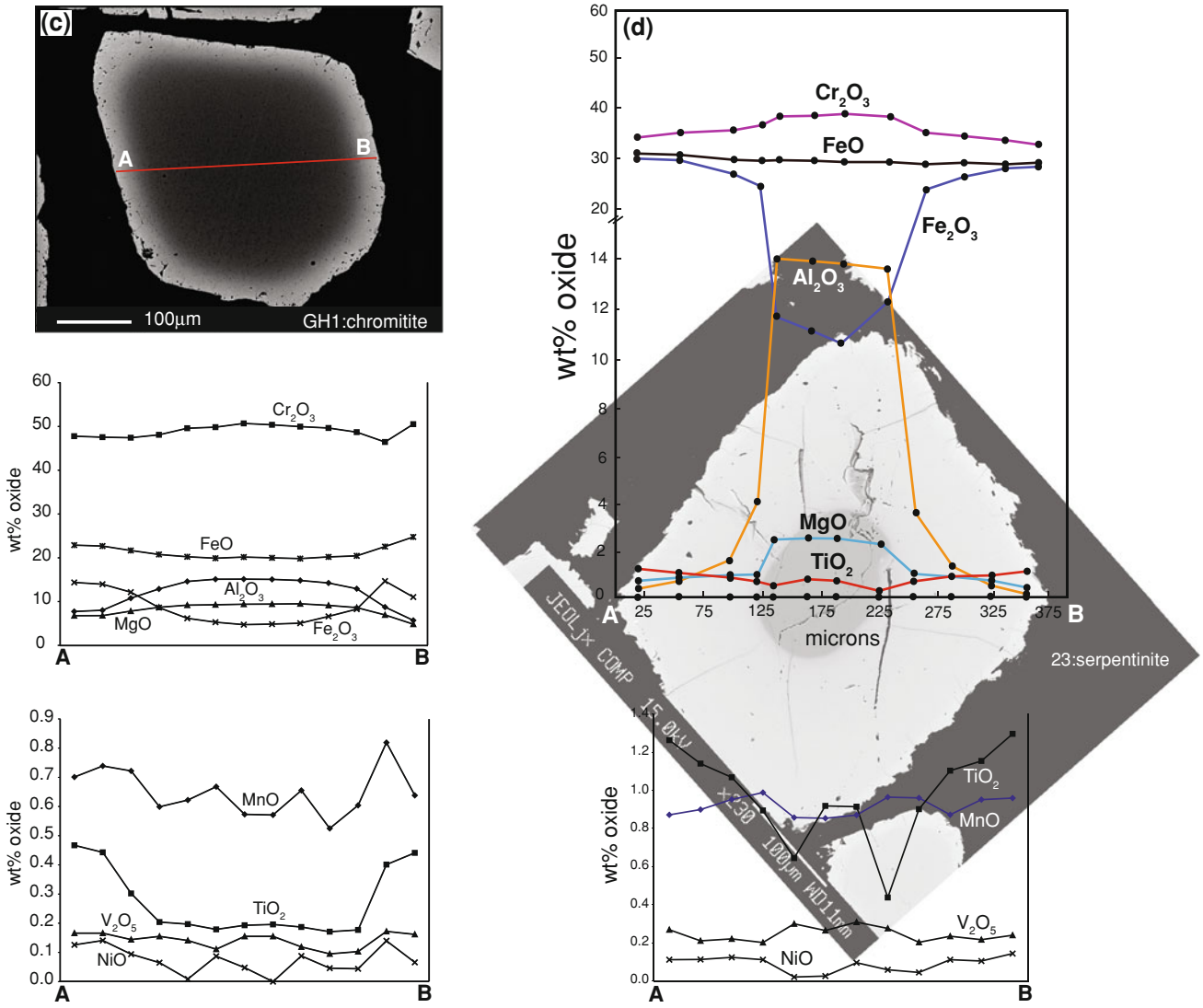

Fig. 6 continued

serpentinite matrix from Nuggihalli with compositions of $Fo_{83–92}$. The olivine grains have variable NiO content that ranges from 0.3 to 0.7 wt%. The interstitial olivine grains in the massive chromitite (sample DHR-27a) have slightly higher NiO content (0.47–0.69 wt%) than in the spotted or net-textured chromitite (0.40–0.59 wt%). The Cr_2O_3 content of the interstitial olivine grains in the net-textured, spotted and schlieren-banded chromitite is lower (0.002–0.08 wt%) than in the massive chromitite (0.1–0.3 wt%; except sample 29B). Pyroxene inclusions are compositionally Mg-rich in the Nuggihalli chromitite with variable Mg-number of 94–99 and Cr_2O_3 content ranging between 0.66 and 2.19 wt% (Electronic Appendix). Very high Mg-number of ~97–99 is observed for the pyroxene inclusions in the massive chromitite from Byrapur. The pyroxene inclusions mainly have augite and pigeonite composition with low wollastonite component. Few pyroxene inclusions represent very refractory compositions (En% ~97–99) presumably due to extreme Fe–Mg exchange with the host chromite grain. Bidyananda and Mitra (2005) had reported interstitial grains that were mainly clinopyroxene (sub-calcic clinopyroxene), with relict orthopyroxene and augite–jadeite intergrowths. The sub-calcic clinopyroxene had a range of Al_2O_3 values from 2.74 to 3.59 wt% with Mg-number of 81–84. The pyroxene grains reported by them were in general slightly titaniferous and sodic with wollastonite content ranging from 26 to 37%.

Chromite

Chromite in various types of chromitite like the massive, net-textured, schlieren-banded and spotted chromitite from Byrapur is both optically and compositionally homogeneous (Fig. 6a). Rarely some outer oxidized parts

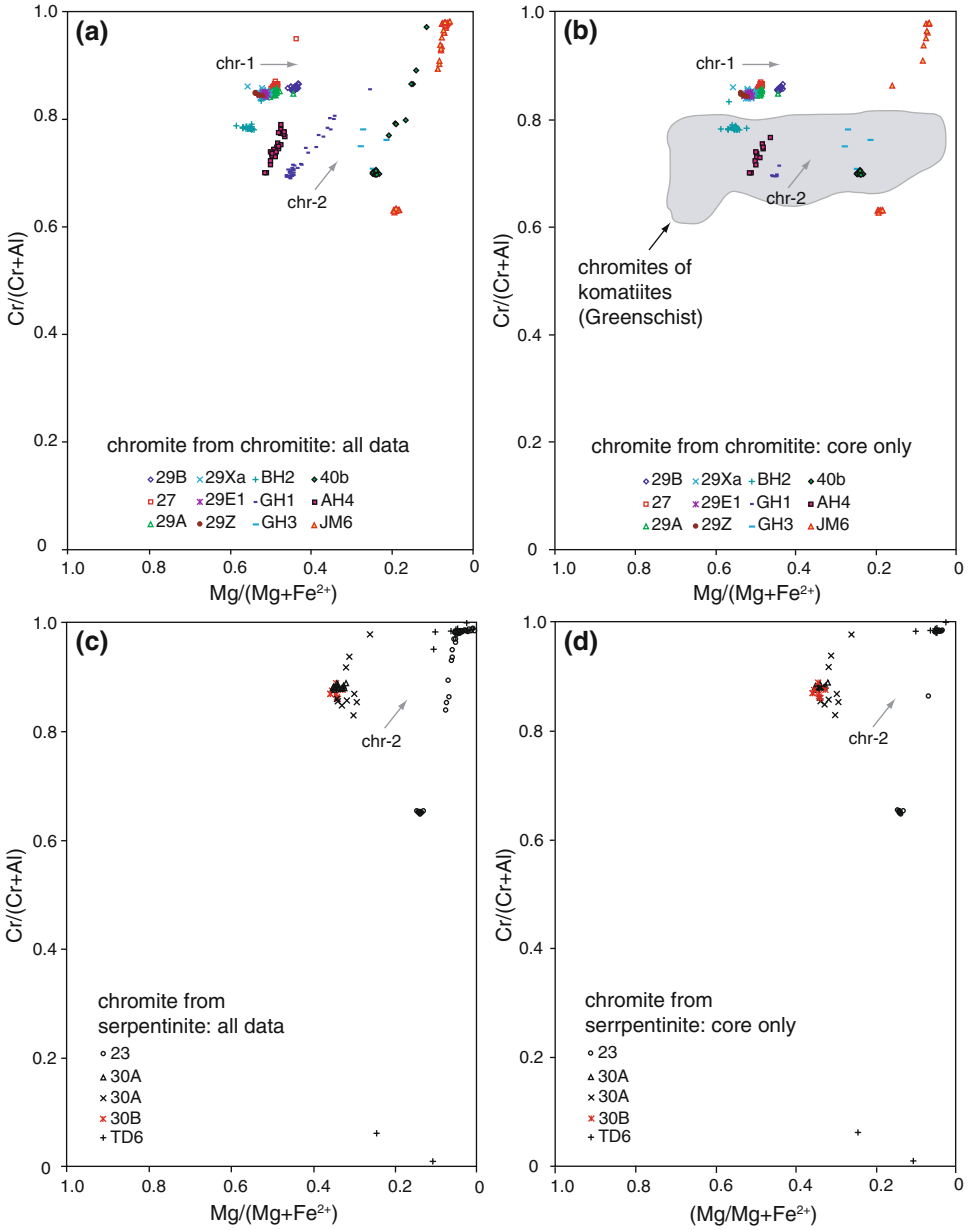

Fig. 7 Variation diagrams illustrating chromite composition. **a** Variation of Cr-ratio plotted against the Mg-ratio in chromitite; *chr-1* trend refers to decreasing magnesium ratio indicating fractional crystallization trend between different varieties of chromitite from Byrapur; *chr-2* trend refers to alteration trend, increasing Cr-ratio is due to loss of Al. **b** Variation of Cr-ratio plotted against the Mg-ratio for chromite cores in chromitite; field of altered chromite in komatiites from greenschist facies is shown; komatiite field—Barnes and Roeder (2001). **c** Variation of Cr-ratio plotted against the Mg-ratio for accessory chromite in serpentinite; chromite shows the alteration trend, *chr-2*. **d** Variation of Cr-ratio plotted against the Mg-ratio for accessory chromite cores in serpentinite; cores are significantly altered and show the alteration trend, *chr-2*. **e** Cr–Al–Fe^{3+} variation of chromite; altered chromite composition plot in the fields of ferritchromit and magnetite (*shaded fields*—Barnes and Roeder 2001). **f** Cr–Al–Fe^{3+} variation of chromite cores (*shaded fields*—Barnes and Roeder 2001). **g** Variation of $Fe^{3+}/(Cr + Al + Fe^{3+})$ ratio plotted against the Mg-ratio for chromite from chromitite and serpentinite; altered chromite shows enrichment of Fe^{3+} content (*shaded field*—Barnes and Roeder 2001). **h**, **i**, **j**, **k** Variation of TiO_2, MnO, V_2O_5 and NiO plotted against the Mg-ratio for chromite in chromitite and serpentinite. **l**, **m** Variation of $Fe^{3+}/(Cr + Al + Fe^{3+})$ ratio plotted against TiO_2 and MnO for chromite in chromitite and serpentinite. Sample details: 27, 29B: massive chromitite, Byrapur; 29A: net-textured chromitite, Byrapur; 29Xa: spotted chromitite, Byrapur; 29E1: schlieren-banded chromitite, Byrapur; 29Z: schlieren-banded chromitite, Byrapur; BH2: massive chromitite, Bhaktarhalli; GH1: massive chromitite, Gobbalahalli; GH3: massive chromitite, Gobbalahalli; 40b: schlieren-banded chromitite, Tagdur (upper ultramafic unit); AH4: massive chromitite, Aladahalli; JM6: chromitite, Jambur; 23: serpentinite, Tagdur (lower ultramafic unit); 30A: serpentinite (chromitite-rich part), Byrapur; 30A: serpentinite, Byrapur; TD6: serpentinite, Tagdur; 30B: serpentinite, Byrapur

Fig. 7 continued

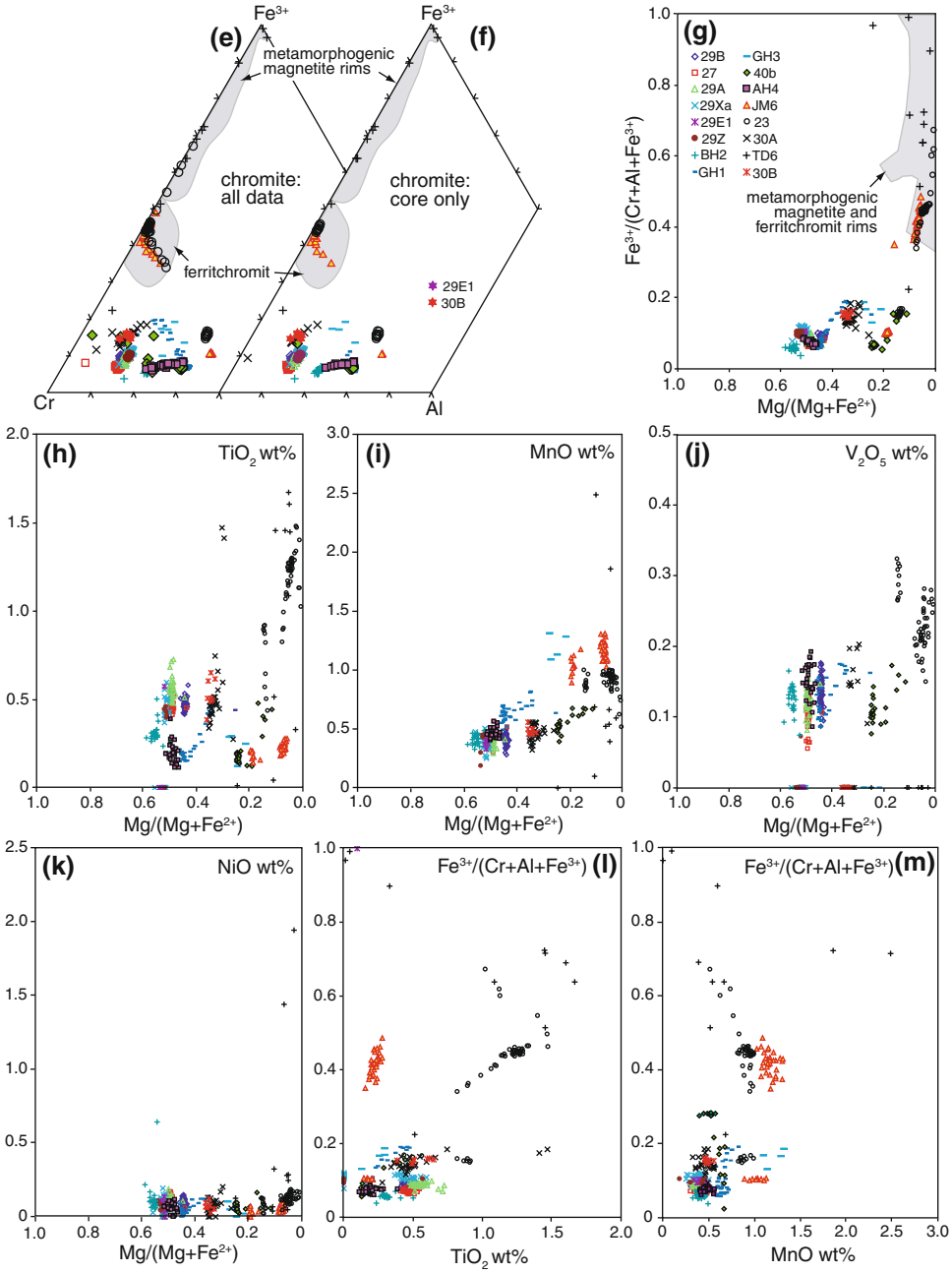

(patches) have been observed that are Fe^{3+}-rich. Chromite from these chromitites shows high and almost constant Cr-ratio (Cr/(Cr + Al) cation ratio) of 0.85–0.86 and a high and variable Mg-ratio (Mg/(Mg + Fe^{2+}) cation ratio) of 0.38–0.58 (Fig. 7a). The cores of these chromite grains show a similar range of values and represent primitive composition (Fig. 7b). The primary compositional variation in the Byrapur chromitite along the Mg/(Mg + Fe^{2+}) axis indicates a fractional crystallization trend (chr-1; Fig. 7a, b), which is commonly observed in layered intrusions (e.g., Rollinson 1995b; Barnes and Roeder 2001). The chromite from Bhaktarhalli (Fig. 2) also represents a chemically and optically homogeneous and unzoned composition, like the chromites from Byrapur (Fig. 7a, b). However, these chromites show higher Mg-ratios and lower Cr-ratios than the chromites from Byrapur. The other chromitite samples exhibit an alteration trend due to Al-loss (chr-2; Fig. 7a, c). Their core compositions show a similar range of values and fall within the field of chromites of komatiites that have been modified by greenschist facies metamorphism (Fig. 7b, d). The wide variation in Cr-ratios due to Al-loss in the accessory chromite in serpentinite (Cr-ratio = 0.02–0.99; Mg-ratio = 0.01–0.38), and silicate-rich chromitite

(Cr-ratio = 0.6–0.99; Mg-ratio = 0.48–0.06), is attributed to intragrain variability or zoning (Figs. 5c, e, f, 6b–d).

In the Cr–Al–Fe^{3+} ternary diagram, three distinct compositional characters are recognized for the Nuggihalli chromite; (1) chemical variation along the Cr–Al side by the modified chromite in the silicate-rich chromitite, (2) chemical variation along the Cr–Fe^{3+} side by the altered chromite from the serpentinite and (3) restricted chemical variation in the unaltered chromite from the massive chromitite of Byrapur and Bhaktarhalli (Fig. 7e, f). The compositions of the accessory chromite in the serpentinite (Tagdur), and the altered chromite from the chromitite, show strong enrichment of Fe^{3+} and fall within the fields of metamorphogenic magnetite rim and ferritchromit (Fig. 7e–g). Some grains are completely altered to ferritchromit such that zoning is not discernible (e.g., samples JM6 and 40b; Figs. 5c, 6b). In these grains, the cores have much higher Cr-ratios than the cores of the zoned chromite in the same sample due to extreme loss of Al during alteration (chr-2; Fig. 7b, d). Overall, the chromite compositions in Nuggihalli are found to vary with respect to location and also within the same sample (Fig. 7).

The accessory chromite in the serpentinite, and the altered grains in the silicate-rich chromitite, shows enrichment in minor elements like TiO_2, MnO and V_2O_5 (Fig. 7h–m). TiO_2 and MnO show negative relations with Mg-ratio but both show variable relations with respect to Fe^{3+}-ratio ($Fe^{3+}/(Cr + Al + Fe^{3+})$ cation ratio) (Fig. 7h, i, l, m). The core and rim of both partly altered and completely altered chromite grains in the silicate-rich chromitite (e.g., sample JM6) show enrichment of TiO_2 (0.16–0.28 wt%), MnO (1.09–1.31 wt%) and Fe^{3+}-ratio (0.35–0.49). TiO_2 shows a positive relation with Fe^{3+}-ratio, and MnO shows a negative relation with the same (Fig. 7l, m). The less altered grains in sample JM6 show restricted variation in composition and low concentration of TiO_2 (0.14–0.17 wt%) and MnO (0.9–1.13 wt%) over constant Fe^{3+}-ratio (0.10–0.11). The accessory chromite grains in the serpentinite generally show similar variations of TiO_2 and MnO with respect to Fe^{3+}-ratios. However, there are some exceptions exhibited by the serpentinites from Tagdur, e.g., samples 23 and TD6 (Fig. 7l, m). The accessory chromite grains in sample 23 show three distinct trends (1) the less altered part (core) of the grain shows slightly variable TiO_2 (0.44–0.91 wt%) over constant Fe^{3+}-ratios (0.15–0.17), (2) the rim or altered part of the same grain shows enrichment of both TiO_2 (0.82–1.48 wt%) and Fe^{3+}-ratios (0.34–0.46) and a distinct positive trend and (3) the completely altered smaller grains from the matrix and the outermost rim of the altered grains show a distinct negative trend (Fig. 7l). Sample TD6 shows wide-scale variation and a negative relation of both TiO_2 and MnO with respect to Fe^{3+}-ratio. The grains that have reached magnetite composition show extremely negligible TiO_2 (0.01–0.04 wt%), and MnO (~0.1 wt%) content, compared to the Fe^{3+}-ratio (0.97–0.99). The unaltered chromite from the massive chromitite of Byrapur shows lower but variable values of the minor elements for constant Mg-ratios, and restricted variation with respect to Fe^{3+}-ratios (Fig. 7h, i, l, m). V_2O_5 shows a variable range over constant Mg-ratios (Fig. 7j), and NiO shows negligible variation in all chromites (Fig. 7k). The compositional trends of the oxides of the minor elements, with respect to Mg-ratio, are comparable with the trends of the metamorphosed accessory chromites in the Archean komatiitic rocks from Kambalda and Windarra of Australia, as described by Barnes (2000). In these settings, increasing values of TiO_2 and MnO are observed with decreasing Mg-ratios and with increasing grades of metamorphism from greenschist to amphibolite facies. However, the variation in the trend of TiO_2 with the degree of alteration in the Nuggihalli chromite grains, as shown in the TiO_2 versus Fe^{3+}-ratio diagram (Fig. 7l), does not conform to the trend of Barnes (2000). In the latter, a simple positive trend of TiO_2 with Fe^{3+}-ratio is observed with increasing metamorphic grade.

Typical igneous chromite from massive chromitites that are genetically linked to komatiitic magma, such as from the Selukwe Railway Block, Zimbabwe, has TiO_2 contents ranging between 0.16 and 0.23 wt% (Mondal et al. 2006). In contrast, the unaltered chromites from the layered intrusions such as the G-chromitite of the Stillwater Complex, Montana, USA, and the UG2 chromitite of the Bushveld Complex, South Africa, have higher TiO_2 contents that range between 0.55–0.67 wt% and 0.47–0.98 wt%, respectively (Mathez and Mey 2005; Mondal et al. 2006). The TiO_2 contents of the unaltered chromite from the massive chromitites of Nuggihalli are similar to the komatiitic chromites from the massive chromitites of the Archean Selukwe Railway Block; however, the altered chromites show significant TiO_2 enrichment, in particular at the rims of the grains.

Compositional zoning in chromite

In order to address the compositional variability of chromite, the zoned chromite grains were studied to determine the element distribution (both major and minor elements) across the grains (Fig. 6). Compositionally homogeneous and unzoned grains were also included in this study for comparison (Fig. 6a). The accessory chromite grains in serpentinite and the altered grains in silicate-rich chromitite exhibit distinct zoning (Fig. 6b, d). The contact between the core and the surrounding ferritchromit rim is very sharp. In contrast, zoning in the altered grains in the silicate-rich massive chromitite is gradational and not sharp (Fig. 6c). The core represents relict chromite composition, which, however, is not pristine and is modified due to oxidation and

metamorphism (Fig. 7b, d, f). The Byrapur chromitites (Figs. 5a, 6a) are exempt from this; the chromites are pristine and show high Mg/Fe and Cr/Al ratios (Fig. 7a, b, e, f, g).

In the zoned grains, Cr_2O_3, Al_2O_3 and MgO show enrichment in the core and progressive loss toward the rim accompanied by strong enrichment of Fe_2O_3 (Fig. 6b, d). FeO shows negligible to minor enrichment toward the rim in the zoned grains (Fig. 6b, d) and in the completely altered grains (Fig. 6b). The major element distribution patterns are comparable with the transitional type-1 chromite of the greenschist facies from Mt. Keith, Australia, and the type-2 zoned chromite of the lower-mid amphibolite facies from Kambalda and Windarra, Australia, as described by Barnes (2000). In the serpentinite, TiO_2 follows the trend of Fe_2O_3 and shows strong enrichment in the rim ($\sim$1.3 wt%). V_2O_5, on the other hand, follows the trend of Cr_2O_3 and shows relative enrichment in the core ($\sim$0.3 wt%; Fig. 6d). Overall, the element distribution patterns of the accessory chromite grains in the serpentinite resemble the distribution patterns of the transitional type-1 chromite of greenschist facies, Mt. Keith, Australia, where lizardite serpentine with stichtite and antigorite–carbonate serpentinite are common lithologies (Barnes 2000). In the altered chromite from the silicate-rich chromitite, no trend is observed for the minor elements other than for MnO, which shows enrichment (0.92–1.2 wt%) in the rim relative to the other minor elements (Fig. 6b). Compositional profiling across optically homogeneous but chemically completely altered grains (smaller grains in Figs. 5c, f, 6b) shows a complementary pattern of distribution between Cr_2O_3 and Fe_2O_3 (Fig. 6b). The compositions of these chromites are similar to the rim of the zoned grains. Chromite in the altered massive chromitite shows complementary pattern of distribution of MgO with FeO, and Cr_2O_3–Al_2O_3 with Fe_2O_3–TiO_2–MnO (Fig. 6c). FeO shows a gradational increase in the rim. TiO_2 shows a distinct trend of progressive enrichment toward the rim ($\sim$0.38–0.47 wt%) that is also followed by MnO ($\sim$0.5–0.7 wt%), but the latter has a variable distribution pattern in the core. In contrast to the zoned grains, the optically homogeneous and unzoned grains (e.g., Byrapur chromitite) show no variation in the major elements and are unaltered (Fig. 6a). They only show slight heterogeneous distributions of the minor elements.

Discussion

Compositional variability of chromite and associated silicate minerals

The olivine inclusions within chromite, and the interstitial olivine grains from different types of chromitites in Nuggihalli, show extremely refractory Fo compositions ($Fo_{96–98}$). The primitive olivine compositions within the Archean greenstone belts are generally in the range of $\sim Fo_{91–95}$, such as in dunite that is genetically linked to high-Mg komatiitic or boninitic magma (Rollinson 1997; Barnes 2006; Mondal et al. 2006). The Fo values of olivine, in the chromitites from Nuggihalli, are more comparable to the interstitial and included olivine ($Fo_{96–98}$) within chromite from the spotted and massive chromitites of the Archean Nuasahi and Sukinda massifs in the Singhbhum Craton, India (Mondal et al. 2006). The Fo values are also comparable with those from the Inyala massive chromitite, Zimbabwe Craton (Rollinson 1997). The refractory Fo compositions of olivine within chromitite are due to subsolidus re-equilibration with chromite. The elevated NiO and Cr_2O_3 concentrations of these olivine grains also indicate re-equilibration during cooling. The higher concentration of Cr_2O_3 in the interstitial olivine grains within massive chromitite compared to the spotted, net-textured, and schlieren-banded chromitite indicates that the modal variation of the associated chromite grains plays an important role in compositionally modifying the olivine grains during subsolidus re-equilibration. This observation is also true for the pyroxene inclusions where subsolidus exchange with the chromite-host causes elevated values of both Cr_2O_3 and Mg-number. The co-existing chromite grains in chromitites, however, do not show much change in their composition as they represent a modally dominant phase. The compositional modification is largest for the included grains as the grains are much smaller in size (Figs. 5a, 6a).

The calculated re-equilibration temperature (Roeder et al. 1979) using chromite–olivine pair (Fo_{96}) from the massive chromitites of Byrapur corresponds to a very low value of around 464–521°C. High-Mg chromites and olivine with compositions of Fo $>$ 90 crystallized at relatively higher temperature (1,250–1,500°C) from komatiitic magma, such as from Kambalda (e.g., Murck and Campbell 1986). If we consider chromite–olivine pairs from other assemblages where modal dominance of chromite and olivine exists individually, such as chromite from massive chromitites (e.g., Bhaktarhalli) and olivine from dunite (serpentinite, as reported by Bidyananda and Mitra 2005), the calculated equilibration temperature then is 1,062°C. Similar calculations for the Archean chromitite deposits such as from Inyala, Zimbabwe (e.g., Rollinson 1997) or from Nuasahi, India (e.g., Mondal et al. 2006) yield equilibration temperatures that are around 885–1,020°C. In contrast, co-existing high-Mg chromite and olivine pairs from all other assemblages of Nuggihalli (e.g., net-textured, spotted and schlieren-banded chromitite) show equilibration temperatures that are significantly low and variable (T = 472–512°C) and similar to the temperatures calculated for the massive chromitites of Byrapur.

This indicates that the chromite–olivine pair in Nuggihalli has re-equilibrated till the serpentinization event.

The compositional contrast, between the accessory chromite grains in the serpentinite and the silicate-rich massive chromitite, is primarily controlled by initial magmatic compositional differences and mode. Later subsolidus re-equilibration and secondary alteration processes caused further compositional diversity. The secondary alteration processes caused oxidation of the accessory chromite grains to ferritchromit and magnetite. The variation in chromite composition between the massive chromitite and the serpentinite-rich part of the same sample is also attributed to initial magmatic compositional differences and subsolidus re-equilibration during alteration. The trend of compositional variability for unaltered and pristine chromite grains from Byrapur along the Fe–Mg axis (Fig. 7a) is due to fractional crystallization; the magma becomes enriched in Fe and Al and shows a decrease in the Mg and Cr contents with progressive evolution. The massive chromitite from Bhaktarhalli represents a more Mg- and Al-rich composition than the ones from Aladahalli, Gobbalahalli and Byrapur and may signify a different parental melt composition. The massive chromitites from Aladahalli and Gobbalahalli have the same range of Mg-ratios, but they are relatively enriched in Al, compared to the massive chromitites from Byrapur. Thus, they may represent a more differentiated part of the magma, although the actual stratigraphic position is very difficult to state (Fig. 7a, b). The compositionally zoned grains show large variations in Cr/Al ratios due to progressive loss of Al to form chlorite during serpentinization. The enrichment of minor elements (e.g., Mn, Ti and V) in the altered parts is related to serpentinization event and later metamorphism of the rocks.

The intensity of alteration in the Nuggihalli chromites was greatly underestimated by the previous workers. Mitra and Bidyananda (2003) calculated the equilibration temperature of around 1,178°C using co-existing olivine–chromite pair. Based on this equilibration temperature, Lenaz et al. (2004) argued that the chromite cores were unaltered and unaffected by metamorphism. In a later study, Bidyananda and Mitra (2005) calculated the temperature of equilibration to be 775–1,080°C and considered this to be the original liquidus temperature. The fO_2 was calculated to be close to the QFM buffer that again indicated magmatic condition. In the Nuggihalli schist belt, two common characteristic trends of compositional variability in chromite are recognized (Fig. 7): one that developed due to fractional crystallization of the magma, and the second that developed due to extensive alteration during serpentinization, and later modification of the grains during low-grade metamorphism. The second trend is very heterogeneous as the composition of chromite is found to differ in a grain, in a section and in hand-specimen scale. Low-grade metamorphism in later stage is largely responsible for homogenizing ferritchromit composition in the grain and for modifying the chromite core.

Ferritchromit formation

Ferritchromit refers to moderately reflecting borders around chromite grains (Bliss and MacLean 1975; Evans and Frost 1975; Burkhard 1993; Barnes 2000), and it represents altered chromite composition. The core in general represents relict chromite that remains as an island amidst the altered rim. In the zoned chromites of Nuggihalli, the composition of the core, however, is perturbed and does not represent the original pristine composition (Fig. 7b, d, f). Overall, the core has higher concentrations of Mg, Cr and Al compared to the rim. The rim shows enrichment of Fe^{3+} and Ti and sometimes Mn, Ni and V (Fig. 6b–d). The Fe^{2+} concentration does not change much across the rim and the core (e.g., Bliss and MacLean 1975; Barnes 2000). There is loss of Cr, Al and Mg from the grain along with simultaneous infiltration of Fe^{3+}, Ti, Ni and Mn. Fluid activity during serpentinization is largely responsible for carrying out this exchange, as fluids are efficient agents of transportation and diffusion. The slower rates of diffusion of the trivalent cations relative to the divalent cations cause a compositional gradient to develop across the chromite grains (e.g., Rollinson 1995b), which we see as zoning. Fluid activity causes incorporation of Mn and Ni from the surrounding olivine grains during serpentinization, while Al and minor Cr are lost to chlorite forming chrome–chlorite (Barnes 2000). Fluids also contribute in bringing about Ti enrichment in the ferritchromit rims and the completely ferritchromitized grains, during serpentinization. The rounded nature of the core indicates that the alteration to ferritchromit had occurred uniformly from all directions (e.g., Bliss and MacLean 1975). The distinct trend of Al-loss followed by loss of Cr and strong enrichment of Fe^{3+}, that is characteristic of ferritchromit (Evans and Frost 1975; Burkhard 1993), is clearly observed in the Cr–Al–Fe^{3+} diagram (Fig. 7e, f). During ferritchromit formation, the Fe^{3+} content of the chromite grains increases due to prevalence of oxidation conditions (Mitra et al. 1992). Devaraju et al. (2007) had also addressed the compositional zoning of the chromite grains in Nuggihalli, where the rim compositions were described to be of ferrian chromite and chromian magnetite, and the core compositions were described to be of aluminium or ferrian chromite.

Formation of ferritchromit has been thought to be linked to either serpentinization process (e.g., Burkhard 1993) or metamorphism in greenschist to lower amphibolite grade (e.g., Bliss and MacLean 1975; Loferski 1986; Barnes

2000). Burkhard (1993) studied the chromites in the serpentinites from the eastern Central Alps and interpreted the alteration of the spinel to be a function of serpentinization and not metamorphism. Metamorphism was thought to cause only re-crystallization of the spinel. Bliss and MacLean (1975) suggested ferritchromit formation to occur by the regional metamorphism of the Precambrian serpentinite, in Central Manitoba. They concluded that serpentinization could not be a sole contributor to ferritchromit formation, as the latter was found to occur in non-serpentinized rocks such as mantle xenoliths and xenocrysts. In the mantle xenoliths, alteration of the chromite to ferritchromit or magnetite is due to magmatic metasomatism by the infiltrating melt. According to Bliss and MacLean (1975), the ferritchromit formation within Precambrian serpentinite was due to a combination of initial serpentinization that caused the development of magnetite rims around chromite, followed by later metamorphism of the assemblage, and reaction of the magnetite rims with the chromite cores to produce the Al- and Mg-poor ferritchromit rim. Loferski (1986) considered the formation of crystallographically controlled intergrowths of ferritchromit plus chlorite, in the accessory chromites of the Red Lodge District, Montana, to be a product of late-stage alteration formed during serpentinization. Extensive formation of ferritchromit occurring along with crystallographically controlled chlorite in the chromite grains, within a breccia zone of the Mesoarchean Nuasahi ultramafic–mafic complex, eastern India is considered to be a product of metasomatism (Mondal and Zhou 2010). Interaction of the chromitite fragments with fluid-rich evolved boninitic magma is considered to have formed the ferritchromit within the Nuasahi breccia zone. Ferritchromit is also common in the serpentinized dunite of the lower ultramafic unit in Nuasahi, which formed during hydrothermal alteration of the ultramafic–mafic complex due to interaction with seawater (Mondal et al. 2003).

In our study, the irregular and patchy occurrences of ferritchromit indicate that no crystallographic orientation has been followed for their formation and that the alteration is heterogeneous (Fig. 5e). These irregular and patchy occurrences probably formed by oxidation in a late hydrothermal episode. This is because the alteration is observed to occur mainly along grain boundaries or fractures through which grain–fluid interaction can easily occur. The serpentinization process itself requires fluid activity, and during this hydrothermal stage the chromite grains are altered. The alteration occurs to be strongest in the accessory chromite grains (Fig. 6d) because the chromites are modally insignificant, and are surrounded by hydrous magnesian silicates (serpentine) with which they can easily exchange cations (Burkhard 1993). Other than serpentinization, metamorphism also plays an important role and cause regular zoning in the chromite grains. There are some grains that show both the regular occurrence of well-developed ferritchromit rims around grain boundary, and the irregular occurrence along fractures (Fig. 5f). Metamorphism causes significant increase in the rates of diffusion of the cations, and this can facilitate the formation of regular and well-developed ferritchromit rims. Metamorphism also enables equilibration of the chromite core with the surrounding silicate assemblages, due to enhanced diffusion (Barnes 2000). The completely ferritchromitized grains in Nuggihalli have been extensively re-equilibrated and homogeneously altered during metamorphism (Figs. 5c, f, 6b). In these grains, the TiO_2 content shows negative correlation with Fe^{3+}-ratios (e.g., sample 23). This indicates either slow diffusion of Ti during metamorphism or their preferential entrapment in Ti-bearing exsolved phases that develop within chromite during metamorphism (e.g., sample TD6; Fig. 5d). The negative correlation of MnO with Fe^{3+}-ratios in the altered part (rim) of the chromite grains, as well as in the completely altered grains, may be attributed to the incorporation of Mn in carbonates which are common within the altered ultramafic rocks.

Compositional modification of the chromite grains depends also on the size of the grain and on the scale of deformation they suffer. The smaller grains are compositionally more modified compared to the larger grains. The same is observed for the highly deformed and fractured chromite grains in the massive chromitites. The intensity and scale of compositional gradient are found to be different in all deposits of the Nuggihalli schist belt. This irregular and heterogeneous nature of variation clearly indicates that ferritchromit formation is definitely related to low temperature hydrothermal alteration of the ultramafic–mafic complex within the schist belt. The secondary processes initiate ferritchromit formation in the grain, and later with increasing grade of metamorphism of the assemblages, the intensity, extent and homogenization of ferritchromit distribution in the chromite grain increases due to increase in the capacity of inter-grain diffusion.

Calculations of parental melt and implications for tectonic settings

The unaltered and primitive chromite compositions, from the chromitites that display limited compositional variability, have been used to compute the parental melt compositions in terms of the FeO/MgO ratio, TiO_2 and Al_2O_3 contents. The Al_2O_3 of the liquid is computed from Maurel and Maurel (1982) for spinel-liquid equilibrium at 1 bar where $(Al_2O_3)_{spinel} = 0.035(Al_2O_3)^{2.42}_{liquid}$. This equation is based on the observation that the Al_2O_3 (wt%) in spinel is a function of Al_2O_3 (wt%) in melt. Kamenetsky

et al. (2001) also showed from the melt inclusion data within chromite from volcanic rocks that there is a linear relationship between the Al_2O_3 and TiO_2 content in chromite, and the Al_2O_3 and TiO_2 content in the melt from which it crystallized. Using the relation of Kamenetsky et al. (2001) from above, the Al_2O_3 content of parental melt for Nuggihalli chromite is obtained. The values of Al_2O_3 of the parental melt calculated from the above methods are found to correspond closely (Table 1). The FeO/MgO ratio of the liquid is computed from the primitive chromite composition using the Maurel and Maurel's (1982) equation, where $\ln(\text{Feo/MgO})_{\text{spinel}} = 0.47 - 1.07Y^{\text{Al}}_{\text{spinel}} + 0.64YFe^{3+}_{\text{spinel}} + \ln(\text{FeO/MgO})_{\text{liquid}}$ where, $Y^{\text{Al}}_{\text{spinel}} = \text{Al}/(\text{Cr} + \text{Al} + Fe^{3+})$ and $Y^{\text{Fe3+}}_{\text{spinel}} = Fe^{3+}/(\text{Cr} + \text{Al} + Fe^{3+})$. The TiO_2 content of the melt is obtained from the melt-TiO_2 versus chromite-TiO_2 diagram of Kamenetsky et al. (2001).

The computed values of Al_2O_3, TiO_2 and FeO/MgO ratio of the melt have been tabulated in Table 1. It is observed that other than the Bhaktarhalli chromitite, the Al_2O_3 content of the melt (8.38–9.1 wt%), calculated from different types of unaltered chromitite from the Nuggihalli schist belt, is more or less similar. The Al_2O_3 value obtained from the Bhaktarhalli massive chromitite is slightly higher (10.51–10.63 wt%). The Al_2O_3 content of the melt is, in general, low and this renders very high Cr-ratios to the unaltered chromite (Fig. 8a). The TiO_2 concentration of the melt is low and is found to range from 0.46 to 0.92 wt%. On comparing the calculated parental melt from this study with primitive magmas from different tectonic settings, our data are found to show closest resemblance with the high-Mg komatiitic basalts of the Archean greenstone belts (Table 1). The calculated composition of the parental melt is similar to the composition of komatiitic rocks reported from the schist belts in the Western Dharwar Craton (Table 1). The chromitite-bearing ultramafic–mafic complex in the Nuggihalli greenstone belt bears close resemblance with the Inyala and Shurugwi greenstone belts of the Zimbabwe Craton, in terms of their field setting and chromite character. They, however, differ significantly in terms of their parental magma character. The parental magma in Nuggihalli possesses lower range of Al_2O_3 and higher FeO/MgO values, than the former, that represents fresh and primary komatiite composition (Table 1).

In Fig. 8a, the primary chromite compositions from the Nuggihalli schist belt are compared with the compositions of chromite from the Archean greenstone belts and the Archean layered complexes. The primary chromites from Byrapur show slightly higher variation in Cr-ratio. Those from Bhaktarhalli are comparable with the compositional range of chromite from the Archean greenstone belts like Selukwe in the Zimbabwe Craton, and the Nuasahi and Sukinda massifs within the early-Archean Iron Ore Group greenstone belt in the Singhbhum Craton, eastern India. In the tectonic discrimination diagram of Cr/(Cr + Al) versus Mg/(Mg + Fe^{2+}) ratio (Fig. 8b) and the Cr–Al–Fe^{3+} ternary diagram (Fig. 8c), the primary chromite compositions from Nuggihalli plot within the field of boninite. In Fig. 8d, compositions of primary spinel from modern volcanic rocks have been used to depict different tectonic settings, as defined by Kamenetsky et al. (2001). In this diagram, the primitive composition of chromites from Nuggihalli and the calculated parental melt, plot within the fields of spinel from the modern back-arc basin and subduction zone (high TiO_2 area).

Calculations indicate high-Mg komatiitic basalt to be the possible parental melt for the Nuggihalli chromites (Table 1), whereas the plots of the primary chromites in tectonic discrimination diagrams suggest derivation from boninitic magma (Fig. 8). Komatiitic basalts are characterized by high SiO_2 for a given MgO, and uniformly low TiO_2, that distinguishes them from modern magmatic products of plumes or mid-ocean ridges. They are considered to have been derived from komatiite by a combination of fractional crystallization and crustal contamination (e.g., Barnes 1989; Grove and Parman 2004). They appear to possess slightly higher TiO_2 than boninites (<0.5%). Boninites are high-SiO_2 (>55%), high-MgO (>9%) lavas, characterized by high compatible trace element contents (Ni ~70–450 ppm, Cr ~200–1,800 ppm) and very low TiO_2 contents (<0.3%) (e.g., Hicky and Frey 1982). Geochemical characters of the boninites are thought to reflect incompatible trace element enrichment of a depleted upper mantle by a subduction-derived fluid or melt, before remelting typically at low pressure (<50 km) within supra-subduction zone settings (Sun et al. 1989). Boninites exclusively occur in modern day supra-subduction zone and back-arc rift settings (Crawford et al. 1989), but they have also been reported from the Hadean, Archean and Proterozoic terrains (Kerrich et al. 1998; Polat et al. 2002; Manikyamba et al. 2005). Parman et al. (2001, 2004) considered that the komatiitic basalts within the Archean greenstone belts are petrographically, geochemically and genetically similar to boninites such as in the Barberton greenstone belt, South Africa. In addition, several workers (e.g., Allègre 1982; Grove et al. 1999; Wilson et al. 2003) have suggested that some komatiites and komatiitic basalts within the greenstone belts resulted from hydrous mantle melting at relatively low temperatures, in supra-subduction settings.

Genesis of chromitite

Formation of massive chromitite requires the parental magma to be saturated with only chromite, relative to other phases, as this would eventually precipitate a monomineralic layer of chromitite. There are various theories that

Table 1 Computed parental melt of the Nuggihalli chromitite calculated from primary chromite compositions and comparison with other ultramafic–mafic magmas

	$Al_2O_{3\ liquid}$ (wt%)	FeO/MgO $_{liquid}$ (wt%)	$TiO_{2\ liquid}$ (wt%)
Nuggihalli greenstone belt, Western Dharwar Craton			
Massive chromitite			
Byrapur-29B	8.56–8.66	1.49–1.55	0.57–0.70
Byrapur-27	8.38–8.63	1.24–1.32	0.57–0.73
Bhaktarhalli-BH2	10.51–10.63	0.94–1.12	0.46–0.57
Spotted chromitite			
Byrapur-29B	8.46–8.7	1.42–1.58	0.57–0.72
Byrapur-29Xa	8.44–9.1	1.18–0.97	0.54–0.73
Net-textured chromitite			
Byrapur-29A	8.59–9.06	1.24–1.33	0.65–0.92
Schlieren-banded chromitite			
Byrapur-29E	8.82–9.05	1.08–1.18	0.55–0.60
Byrapur-29Z	8.9–9.05	1.04–1.12	0.79
Parental melt calculated using Kamenetsky et al. (2001)	ca 8.39		ca 0.63
Archean greenstone belts, Zimbabwe Craton			
Massive chromitite			
Inyala, Zimbabwe[a]	11.04–11.11	0.45–0.46	
Selukwe, Zimbabwe[a]	11.78–12.23	0.56–0.60	
Prince mine, Zimbabwe[b]	10.49–11.92	0.02–0.36	
Rhonda, Zimbabwe[b]	11.16–11.89	0.61–0.78	
IOG greenstone belts, Singhbhum Craton[c]			
Massive chromitite			
Nuasahi massif	10.3–11.0	0.29–0.71	
Sukinda massif	10.2–11.5	0.68–0.84	
Archean Large Layered Intrusion[c]			
Stillwater G-chromitite	12.3–12.6	1.48–1.58	
Ophiolitic chromitite[c]			
Oman chromitite	11.4–16.4	0.62 ± 0.02	0.23–0.92
IOG high-Mg basalts, Singhbhum Craton[c]			
Nuasahi area	7.9	0.52	
Sukinda area	10.7	0.94	
Gorumahisani-Badampahar area	8.8	0.91	
Archean low-Ti siliceous high-Mg basalts[d]			
Barberton	12.7–13.4	0.74	0.31–0.33
Pilbara	10.1–11.7	0.58–0.75	0.39–0.43
Komatiitic basalts, Archean greenstone belts			
Tisdale township, Abitibi greenstone belt[e]	8.58–9.38	0.74–0.85	0.53–0.57
J.C. Pura belt, Western Dharwar Craton[f]	8.91	0.66	0.46
Kalyadi belt, Western Dharwar Craton[f]	7.9	0.66	0.40
Archean Boninites[g]			
Gadwal greenstone belt, Eastern Dharwar Craton	8.78–14.10	0.48–0.96	0.24–0.36
Phanerozoic Boninites			
Bonin island, Japan[h]	10.6–14.4	0.7–1.4	0.10–0.52
Tonga trench[i]	11.29–14.87	0.68–0.89	0.22–0.30
Layered Intrusions (parent magma)[c]			
Bushveld (Average 'U' Type)	11.5	0.74	
Great Dyke	11.1	0.61	

[a] Computed using chromite data from Rollinson (1997)
[b] Computed using chromite data from Prendergast (2008)
[c] Mondal et al. (2006 and references therein)
[d] Barnes (1989 and references therein)
[e] Fan and Kerrich (1997)
[f] Jayananda et al. (2008)
[g] Manikyamba et al. (2005)
[h] Hicky and Frey (1982)
[i] Falloon et al. (2008)

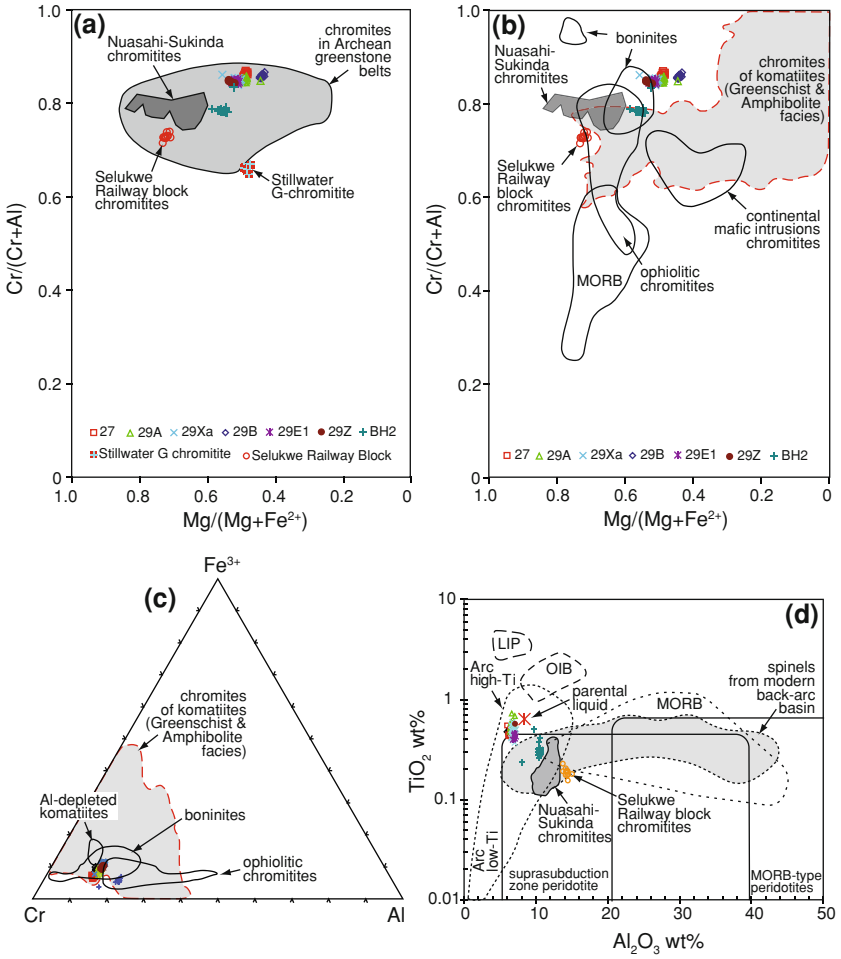

Fig. 8 Tectonic discrimination diagrams. **a** Variation of Cr-ratio and Mg-ratio of primary chromite compositions from the Nuggihalli schist belt; chromite from other Archean occurrences is shown for comparison. *Shaded field*—Rollinson (1995b); data of different chromites from other localities—Mondal et al. (2006). **b** Cr-ratio and Mg-ratio variations of primary chromite compositions from the Nuggihalli schist belt compared with chromite compositions from different types of magmas, ophiolitic chromitites and continental mafic intrusions chromitites. *Shaded field*—Barnes and Roeder (2001); data of Nuasahi–Sukinda chromitite and Selukwe chromitite—Mondal et al. (2006). **c** Trivalent cation plot of primary chromite compositions from the Nuggihalli schist belt. Fields of chromite associated with boninite, Al-depleted komatiite, ophiolite and altered greenschist komatiite are shown for comparison. *Different fields*—Barnes and Roeder (2001). **d** TiO_2–Al_2O_3 variation in Cr-spinel with respect to modern day tectonic settings; fields—Kamenetsky et al. (2001). See Fig. 7 for sample details

have been proposed to explain the above phenomenon such as increase in total pressure (Cameron 1977; Lipin 1993), fO_2 (Cameron and Desborough 1969; Ulmer 1969; Murck and Campbell 1986) and $aSiO_2$ through contamination (Irvine 1975). However, the most acceptable theory is that of magma mixing model proposed by Irvine (1977). All these existing models of chromitite formation have been recently reviewed by Mondal and Mathez (2007), and the reader is referred to their paper for an in-depth analysis of the different hypotheses and their applicability.

The magma mixing model (Irvine 1977) explained that the mixing of a chemically primitive mafic melt with a more evolved mafic melt can cause the hybrid magma to be supersaturated with chromite alone; thus, a monomineralic chromitite layer would eventually form by subsequent settling. This is due to the curved nature of the olivine–chromite cotectic in the MgO–Cr_2O_3–SiO_2 system. The hybrid magma is expected to be less differentiated than the originally evolved magma present in the magma chamber prior to mixing. This would result in variation in the Mg/Fe ratios within the entire sequence; the rocks above the chromitite layer are expected to possess greater Mg/Fe ratios than the ones below it. Furthermore, mixing of two magmas with different fO_2 and temperature is also expected to produce a hybrid magma supersaturated in chromite (e.g., Murck and Campbell 1986). In the Nuggihalli schist belt, the host peridotitic rocks for the massive chromitite are extensively altered to serpentinite. Therefore, there is little scope to test the magma mixing model for the studied chromitites. However, there are indications for the

presence of slightly different melt compositions that may support the mixing model (as inferred from Bhaktarhalli chromite; Fig. 7a, b; Table 1). Contamination or assimilation of mafic magmas caused by felsic roof rocks had been proposed by Irvine (1975) as the probable mechanism of chromitite formation; however, he eventually rejected this idea (Irvine 1977).

Water can also play an important role for chromitite formation in the supra-subduction settings (e.g., Mondal et al. 2006). Experiments by Ford et al. (1972), Sisson and Grove (1993), and Gaetani et al. (1994) showed that the effect of high water concentration on cooling mafic magma is to stabilize the oxide phases on the liquidus relative to the silicate phases, thereby causing chromite to be the first phase on the liquidus to crystallize (Nicholson and Mathez 1991; Bannister et al. 1998; Mathez and Mey 2005). Gaetani et al. (1994) showed that by changing the water pressure from 1 atm (dry) to 200 MPa, chromite becomes the first phase to appear on the liquidus, and its stability field is also greatly enhanced. The formation of the monomineralic chromitite bodies in the Nuggihalli schist belt may be due to a combination of magma mixing involving a boninitic or high-Mg komatiitic basaltic magma, coupled with relatively high water contents of the mixed magma in a supra-subduction zone setting.

Formation of thick and extensive chromitite bodies such as in the Bushveld Complex, South Africa, has been explained by the accumulation of chromite from a magma in which chromite crystals were suspended (Mondal and Mathez 2007). The proposition is based on the observations that with respect to chromitites, the Bushveld Complex contains far more chromite than can be accounted for by the apparent mass of the present body (e.g., Eales 2000), and that the massive chromitite layers, such as the UG2 chromitite, are hosted within orthopyroxenite having uniform and similar orthopyroxene compositions both above and below (Mondal and Mathez 2007). Crystal laden magmas are common in lavas and hypabyssal rocks (e.g., Marsh 1996) and within the magma conduit systems (e.g., Sinton and Detrick 1992). Calculations by Mondal and Mathez (2007) based on modal abundances of chromite showed that the Bushveld chromitite could have been produced by crystal accumulation from geologically reasonable amounts of magma. Similarly, the chromitite bodies in the Nuggihalli schist belt may be formed as intrusives from chromite crystal slurry, because the amount of chromites are much higher than the overall mass of the ultramafic bodies in the belt. However, the present configurations of the chromitite bodies, including the host ultramafic rocks, are due to multiphase deformation processes that are common in the greenstone belts.

Conclusions

The main conclusions of this study are

1. Strong compositional variability is exhibited by the chromites from the Nuggihalli schist belt in the form of subsolidus readjustment of composition and oxidation to ferritchromit. Primary chromite composition is only retained by the massive chromitite from Byrapur that shows high magnesium and chromium ratio.
2. Sub-solidus re-equilibration is related to mode and is responsible for developing extremely refractory composition of the olivine and pyroxene phases (both interstitial and included) within massive chromitite, without causing any effect on chromite composition. Compositional differences between the chromites in massive chromitite, and in serpentinite and silicate-rich chromitite, are also attributed to sub-solidus adjustments.
3. Alteration and oxidation of the chromite grains develop zoning where the rim is ferritchromit and the core composition is modified (except for Byrapur chromites). Some grains do not show zoning but are completely altered to either ferritchromit or magnetite. Secondary hydrothermal processes initiate ferritchromit formation, and later low-grade metamorphism is largely responsible for homogenizing their distribution across the entire grain.
4. The parental magma of the Nuggihalli chromitite is represented by a high-Mg komatiitic basalt, which is calculated from unaltered chromite composition. Tectonic discrimination plots indicate parental melt to be boninitic, from supra-subduction setting.
5. Formation of the thick chromitite bodies in the Nuggihalli schist belt may be due to a combination of magma mixing involving a boninitic or high-Mg komatiitic basaltic magma, coupled with relatively high water contents of the mixed magma. Intrusion of chromite crystal laden magma is another possibility; however, there is little scope to test these hypotheses.

Acknowledgments Karnataka State Mining Corporation, India, is acknowledged for logistical support and all help to RM and SKM during field work. M. Lingadevaru, T. C. Devaraju and K. S. Anantha Murthy are acknowledged for guidance and support during field work. SKM is grateful to Tod Waight and Alfons Berger for help during EPMA work and Hanne Lambert, GEUS (GEOCENTER, Copenhagen) for help during section preparation. We are grateful to Ahmed H. Ahmed and an anonymous reviewer for constructive and thoughtful comments on this article. John Bowles and Ed Mathez are acknowledged for informal review of this article with thoughtful comments and editorial suggestions on the text. We are thankful to Tim Grove for his editorial comments on this article.

References

Abzalov MZ (1998) Chrome spinels in gabbro-wehrlite intrusions of the Pechenga area, Kola Peninsula, Russia: emphasis on alteration features. Lithos 43:109–134

Allègre CJ (1982) Genesis of Archean komatiites in a wet ultramafic subducted plate. In: Arndt NT, Nisbet EG (eds) Komatiites. George Allen and Unwin, London, pp 495–500

Bannister V, Roeder P, Poustovetov A (1998) Chromite in the Paricutin lava flows (1943–1952). J Volcanol Geotherm Res 87:151–171

Barnes SJ (1989) Are Bushveld U-type parent magmas boninites or contaminated Komatiites? Contrib Mineral Petrol 101:447–457

Barnes SJ (2000) Chromite in Komatiites. II. Modification during greenschist to mid-amphibolite facies metamorphism. J Petrol 41:387–409

Barnes SJ (2006) Komatiites: petrology, volcanology, metamorphism, and geochemistry. Econ Geol Special Publication 13, pp 13–49

Barnes SJ, Roeder PL (2001) The range of spinel compositions in terrestrial mafic and ultramafic rocks. J Petrol 42:2279–2302

Bidyananda M, Mitra S (2005) Chromitites from komatiitic affinity from the Archean Nuggihalli greenstone belt in South India. Mineral Petrol 84:169–187

Bidyananda M, Deomurari MP, Goswami JN (2003) ^{207}Pb-^{206}Pb ages of zircon from the Nuggihalli schist belt, Dharwar craton, southern India. Curr Sci 85:1482–1485

Bliss NW, MacLean WH (1975) The paragenesis of zoned chromite from central Manitoba. Geochim Cosmochim Acta 39:973–990

Burkhard DJM (1993) Accessory chromian spinels: their coexistence and alteration in serpentinites. Geochim Cosmochim Acta 57:1297–1306

Cameron EN (1977) Chromite in the central sector of the eastern Bushveld Complex, South Africa. Am Mineral 62:1082–1096

Cameron EN, Desborough GA (1969) Occurrence and characteristics of chromite deposits, eastern Bushveld Complex. Econ Geol Monogr 4:23–40

Crawford AJ, Falloon TJ, Green DH (1989) Classification, petrogenesis and tectonic setting of boninites. In: Crawford AJ (ed) Boninites. Unwin and Hyman, London, pp 2–44

Damodaran KT, Somasekar B (1976) Chrome chlorite (kotschubeite) from the Nuggihalli schist belt. Clays Clay Miner 24:31–35

De Wit MJ, Ashwal LD (1995) Greenstone belts: what are they? S Afr J Geol 98(4):505–520

Devaraju TC, Alapieti TT, Kaukonen RJ, Sudhakara TL (2007) Chemistry of Cr-spinels from ultramafic complexes of western Dharwar craton and its petrogenetic implications. J Geol Soc India 69:1161–1175

Devaraju TC, Viljoen RP, Sawkar RH, Sudhakara TL (2009) Mafic and ultramafic magmatism and associated mineralization in the Dharwar craton, southern India. J Geol Soc India 73:73–100

Dick HJB, Bullen T (1984) Chromian spinel as a petrogenetic indicator in abyssal and alpine-type peridotites and spatially associated lavas. Contrib Mineral Petrol 86:54–76

Droop GTR (1987) A general equation for estimating Fe^{3+} concentrations in ferromagnesian silicates and oxides from microprobe analysis, using stoichiometric criteria. Mineral Mag 51:431–435

Eales HV (2000) Implications of the chromium budget of the Western Limb of the Bushveld Complex. S Afr J Geol 103:141–150

Evans BW, Frost BR (1975) Chrome-spinel in progressive metamorphism—a preliminary analysis. Geochim Cosmochim Acta 39:959–972

Falloon TJ, Danyushevsky LV, Crawford AJ, Meffre S, Woodhead JD, Bloomer SH (2008) Boninites and adakites from the northern termination of the Tonga Trench: implications for adakite petrogenesis. J Petrol 49:697–715

Fan J, Kerrich R (1997) Geochemical characteristics of aluminum depleted and undepleted komatiites and HREE-enriched low-Ti tholeiites, western Abitibi greenstone belt: a heterogeneous mantle plume-convergent margin environment. Geochim Cosmochim Acta 61:4723–4744

Ford CE, Bigger GM, Humphries DJ, Wilson G, Dixon D, O'Hara MJ (1972) Role of water in the evolution of the lunar crust; an experimental study of sample 14310; an indication of lunar calc-alkaline volcanism. In: Proceedings of third lunar science conference, geochimica et cosmochimica acta supplement 1, pp 207–229

Gaetani GA, Grove TL, Bryan WB (1994) Experimental phase relations of basaltic andesite from hole 839B under hydrous and anhydrous conditions. In: Hawkins J, Parson L, Allan J (eds) Proceedings of the ocean drilling Program, scientific results 135, pp 557–563

Grove TL, Parman SW (2004) Thermal evolution of the earth as recorded by komatiites. Earth Planet Sci Lett 219:173–187

Grove TL, Parman SW, Dann JC (1999) Conditions of magma generation for Archean komatiites from the Barberton Mountainland, South Africa. In: Fei Y, Bertka CM, Mysen BO (eds) Mantle petrology; field observations and high-pressure experimentation; A tribute to Francis R (Joe) Boyd. Geochemical Society Publication 6, pp 155–167

Gupta S, Rai SS, Prakasam KS, Srinagesh D (2003) The nature of the crust in southern India: implications for Precambrian crustal evolution. Geophys Res Lett 30:1419. doi:10.1029/2002GL016770

Hamlyn PR, Keays RR (1979) Origin of chromite compositional variation in the Panton Sill, Western Australia. Contrib Mineral Petrol 69:75–82

Hicky RL, Frey FA (1982) Geochemical characteristics of boninite series volcanics: implications for their source. Geochim Cosmochim Acta 46:2099–2115

Irvine TN (1965) Chromian spinel as a petrogenetic indicator. Part I, Theory. Can J Earth Sci 2:648–671

Irvine TN (1967) Chromian spinel as a petrogenetic indicator. Part II, Petrographic applications. Can J Earth Sci 4:71–103

Irvine TN (1975) Crystallization sequences in the Muskox intrusion and other layered intrusions-II. Origin of chromitite layers and similar deposits of other magmatic ores. Geochim Cosmochim Acta 39:991–1020

Irvine TN (1977) Origin of chromitite layers in the Muskox intrusion and other layered intrusions: a new interpretation. Geology 5:273–277

Jackson ED (1969) Chemical variation in coexisting chromite and olivine in chromitite zones of the Stillwater complex. Econ Geol Monogr 4:41–71

Jafri SH, Khan N, Ahmed SM, Saxena R (1983) Geology and geochemistry of Nuggihalli schist belt, Dharwar craton, Karnataka, India. In: Naqvi SM, Rogers JJW (eds) Precambrian of South India. Memoir Geol Soc India No 4, pp 110–120

Jayananda M, Kano T, Peucat JJ, Channabasappa S (2008) 3.35 Ga komatiite volcanism in the western Dharwar craton, southern India: constraints from Nd isotopes and whole-rock geochemistry. Precambrian Res 162:160–179

Kamenetsky VS, Crawford AJ, Meffre S (2001) Factors controlling chemistry of magmatic spinel: an empirical study of associated olivine, Cr-spinel and melt inclusions from primitive rocks. J Petrol 42:655–671

Kerrich R, Wyman D, Fan J, Bleeker W (1998) Boninite series; low Ti-tholeiite associations from the 2.7 Ga Abitibi greenstone belt. Earth Planet Sci Lett 164:303–316

Leelananadam C, Burke K, Ashwal LD, Webb SJ (2006) Proterozoic mountain building in Peninsular India: an analysis based primarily on alkaline rock distribution. Geol Mag 143:1–18

Lenaz D, Andreozzi GB, Mitra S, Bidyananda M, Princivalle F (2004) Crystal chemical and 57Fe Mössbauer study of chromite from the Nuggihalli schist belt (India). Mineral Petrol 80:45–57

Lipin BR (1993) Pressure increases in the formation of chromite seams and the development of the ultramafic series in the Stillwater complex, Montana. J Petrol 34:955–976

Loferski PJ (1986) Petrology of metamorphosed chromite bearing rocks from the Red Lodge District, Montana. US Geol Surv Bull 1626-B:B1–B34

Loferski PJ, Lipin BR (1983) Exsolution in metamorphosed chromite from the Red Lodge district, Montana. Am Mineral 68:777–789

Manikyamba C, Naqvi SM, Rao DVS, Mohan MR, Khanna TC, Rao TG, Reddy GLN (2005) Boninites from the Neoarchaean Gadwal Greenstone belt, eastern Dharwar Craton, India: implications for Archaean subduction processes. Earth Planet Sci Lett 230:65–83

Marsh B (1996) Solidification fronts and magmatic evolution. Mineral Mag 60:5–40

Mathez EA, Mey JL (2005) Character of the UG2 chromitite and host rocks and petrogenesis of its pegmatoidal footwall, northeastern Bushveld complex. Econ Geol 100:1617–1630

Maurel C, Maurel P (1982) Etude expérimentale de la solubilité du chrome dans les bains silicatés basiques et sa distribution entre liquide et minéraux coexistants: conditions d'existence du spinelle chromifére. Bull Minéral 105:197–202

Mitra S, Bidyananda M (2001) Crystallochemical characteristics of chlorites from the greenstone belt of south India and their geothermometric significance. Clay Sci 11:479–501

Mitra S, Bidyananda M (2003) Evaluation of metallogenic potential of the Nuggihalli greenstone belt, South India. C R Geosci 335:185–192

Mitra S, Pal T, Maity PK, Moon HS (1992) Ferritchromit and its optochemical behavior. Mineral J 16:173–186

Mondal SK (2009) Chromite and PGE deposits of Mesoarchaean ultramafic-mafic suites within the greenstone belts of the Singhbhum craton, India: implications for mantle heterogeneity and tectonic setting. J Geol Soc India 73:36–51

Mondal SK, Mathez EA (2007) Origin of the UG2 chromitite layer, Bushveld complex. J Petrol 48:495–510

Mondal SK, Zhou M-F (2010) Enrichment of PGE through interaction of evolved boninitic magmas with early formed cumulates in a gabbro-breccia zone of the Mesoarchean Nuasahi massif (eastern India). Miner Depos 45:69–91

Mondal SK, Baidya TK, Rao KNG, Glascock MD (2001) PGE and Ag mineralization in a breccia zone of the Precambrian Nuasahi ultramafic-mafic complex, Orissa, India. Can Mineral 39:979–996

Mondal SK, Ripley EM, Li C, Ahmed AH, Arai S, Liipo J, Stowe C (2003) Oxygen isotopic compositions of Cr-spinels from Archean to Phanerozoic chromite deposits. Goldschmidt conference at Japan, Abstract with program, Abstract published in Geochim Cosmochim Acta, vol 18S, p A301

Mondal SK, Ripley EM, Li C, Frei R (2006) The genesis of Archean chromitites from the Nuasahi and Sukinda massifs in the Singhbhum craton, India. Precambrian Res 148:45–66

Mondal SK, Mukherjee R, Rosing MT, Frei R, Waight T (2008) Petrologic, geochemical and isotopic study of 3.1 Ga peridotite-chromitite suite from the western Dharwar craton (India): evidence for recycling of oceanic crust in the Mesoarchean. Eos Trans AGU 89(53), Fall Meet Suppl, Abstract V33C-2237

Murck BN, Campbell IH (1986) The effects of temperature, oxygen fugacity and composition on the behavior of chromium in basic and ultramafic melts. Geochim Cosmochim Acta 50:1871–1887

Murthy NGK (1987) Mafic dyke swarms of the Indian shield, Mafic swarms. Geol Assoc Canada special paper 34, pp 393–400

Naqvi SM (2005) Geology and evolution of the Indian plate (Hadean to Holocene—4 Ga to 4Ka). Capital, New Delhi, p 450

Nicholson DM, Mathez EA (1991) Petrogenesis of the Merensky Reef in the Rustenburg section of the Bushveld complex. Contrib Mineral Petrol 107:293–309

Nijagunappa R, Naganna C (1983) Nuggihalli schist belt in the Karnataka craton: an Archaean layered complex as interpreted from chromite distribution. Econ Geol 79:507–513

Papp JF (2008) Chromium-2006. In: USGS minerals yearbook 2006, pp 17.1–17.22

Parman SW, Grove TL, Dann JC (2001) The production of Barberton komatiites in an Archean subduction zone. Geophys Res Lett 28:2513–2516

Parman SW, Grove TL, Dann JC (2004) A subduction model for komatiites and cratonic lithosphere mantle. S Afr J Geol 107:107–118

Polat A, Hofmann AW, Rosing MT (2002) Boninite-like volcanic rocks in the 3.7–3.8 Ga Isua greenstone belt, West Greenland: geochemical evidence for intra-oceanic subduction zone processes in the early earth. Chem Geol 184:231–254

Prendergast MD (2008) Archean komatiitic sill-hosted chromite deposits in the Zimbabwe Craton. Econ Geol 103:981–1004

Radhakrishna BP (1983) Archean granite-greenstone terrain of the south Indian shield. In: Naqvi SM, Rogers JJW (eds) Precambrian of South India. Memoir Geol Soc India No 4, pp 1–46

Radhakrishna BP (1996) Mineral resources of Karnataka. Geol Soc India, Bangalore, p 471

Radhakrishna BP, Naqvi SM (1986) Precambrian continental crust of India and its evolution. J Geol 94:145–166

Radhakrishna BP, Vaidyanadhan R (1994) Geology of Karnataka. Geol Soc India, Bangalore, p 298

Ramakrishnan M (1981) Nuggihalli and Krishnarajpet belts. In: Swami Nath J, Ramakrishnan M (eds) Early Precambrian supracrustals of southern Karnataka. Geol Surv India Mem No 112, pp 61–70

Ramakrishnan M (2009) Precambrian mafic magmatism in the western Dharwar craton, Southern India. J Geol Soc India 73:101–116

Roeder PL, Campbell IH, Jamieson HE (1979) A re-evaluation of the olivine-spinel geothermometer. Contrib Mineral Petrol 68:325–334

Rollinson H (1995a) Composition and tectonic settings of chromite deposits through time. Econ Geol 90:2091–2092

Rollinson H (1995b) The relationship between chromite chemistry and the tectonic setting of Archean ultramafic rocks. In: Blenkinsop TG, Tromps P (eds) Sub-Saharan Econ Geol Amsterdam, Balkema, pp 7–23

Rollinson H (1997) The Archaean komatiite-related Inyala chromitite, Southern Zimbabwe. Econ Geol 92:98–107

Scowen PAH, Roeder PL, Helz RT (1991) Reequilibration of chromite within Kilauea Iki lava lake, Hawaii. Contrib Mineral Petrol 107:8–20

Sinton JM, Detrick RS (1992) Mid-ocean ridge magma chambers. J Geophys Res 97(B):197–216

Sisson TW, Grove TL (1993) Experimental investigations of the role of H_2O in calc-alkaline differentiation and subduction zone magmatism. Contrib Mineral Petrol 113:143–166

Stowe CW (1987) Chromite deposits of the Shurugwi greenstone belt, Zimbabwe. In: Stowe CW (ed) Evolution of chromium ore fields. Van Nostrand Reinhold, New York, pp 71–88

Stowe CW (1994) Compositions and tectonic settings of chromite deposits though time. Econ Geol 89:528–546

Sun SS, Nesbitt RW, McCulloch MT (1989) Geochemistry and petrogenesis of Archaean and early Proterozoic siliceous high-magnesian basalts. In: Crawford AJ (ed) Boninites and related rocks. Unwin and Hyman, London, pp 148–173

Ulmer GC (1969) Experimental investigations of chromite spinels. Econ Geol Monogr 4:114–131

Wilson AH, Shirey SB, Carlson RW (2003) Archean ultradepleted komatiites formed by hydrous melting of cratonic mantle. Nature 423:858–861